Use of Inducible, Selectable and Stable Fluorescent Protein-Tagged 5-HT2 Receptors in Elucidating JC Polyomavirus Cellular Entry and Trafficking

A thesis submitted in partial fulfillment of the requirements for the degree of Bachelor of Science with Honors in the Neuroscience concentration of Brown University

Abigail Atkinson
Author

Walter Atwood
Thesis Advisor

Acknowledgements

I would like to express my deep gratitude to everyone who assisted, guided, or mentored me throughout the duration of this project. In particular, I would like to thank Dr. Walter Atwood for his excellent advising and mentorship throughout the entirety of my time working with him. The ways I have learned to think about science through discussions with him will forever shape the research I conduct. In addition, I would like to thank Dr. Benedetta Assetta for her exceedingly helpful mentorship throughout this project. It was through Dr. Assetta that I became the scientist I am today; I would not have accomplished everything I did without her experience and creativity to guide me. I would like to thank the entire Atwood lab for their amazing support, guidance and energy; Dr. Bethany O'Hara, Dr. Gretchen Gee, Dr. Sheila Haley and Jenna Morris-Love all contributed greatly to my ability to accomplish this project. I would like to thank Kevin Carlson and the Brown University Flow Cytometry Facility for their assistance with cell sorting. I would like to thank Geoff Williams and the Brown University Leduc Bioimaging Facility for the training and equipment necessary for this project. I would like to thank the Karen T. Romer Undergraduate Teaching and Research Award Committee for funding summer research to work on this project. I would like to thank the Brown University Transportation Office for providing transportation to the laboratory. Finally, I would like to thank the Brown University Neuroscience Department and the Brown University Molecular Biology, Cell Biology and Biochemistry departments.

Abstract

Use of Inducible, Selectable and Stable Fluorescent Protein-Tagged 5-HT2 Receptors in Elucidating JC Polyomavirus Cellular Entry and Trafficking

JC Polyomavirus (JCPyV) is a human pathogen which in immunocompromised individuals causes progressive multifocal leukoencephalopathy (PML), a fatal central nervous system disease. All three variants of serotonin subtype 2 receptors (5-HT2Rs) are important for JCPyV infection of glial cells, but little is known about how the receptors and virus interact. This study generated inducible lentiviral vectors expressing the 5-HT2R proteins linked to C-terminal (intracellular) fluorescent protein tags, which provided a platform for specific tracking of receptor location. Stable cell lines containing 5-HT2AR-BFP, 5-HT2BR-mCherry and/or 5HT2CR-EGFP were evaluated for receptor functionality and used to begin exploring how JCPyV interacts with 5-HT2Rs during entry into host cells. Two of the three modified receptors were expressed evenly over the cell membrane and responded to addition of receptor ligand as expected, suggesting that the protein tag did not generally alter receptor functionality. Confocal microscopy was used to evaluate potential heterodimerization between JCPyV and modified 5-HT2R subtypes, but additional data is needed to determine whether the results are significant. Elucidating the role of 5-HT2Rs in JCPyV infection through these cells may lead to the identification of drug targets or therapies to treat or prevent PML.

Contents

Introduction

Pathophysiology and Epidemiology of Infection

Viruses in the family *Polyomaviridae*, called polyomaviruses for their occasional role in tumor development, are found across a wide range of host species (Pinto et al. 2014). Since the first polyomavirus was isolated in 1952 and identified as murine K virus, no fewer than 73 disparate polyomaviruses have been identified, 13 of which are found in humans (Killham 1952, Haley and Atwood 2017). JC polyomavirus (JCPyV) and BK polyomavirus (BKPyV), the first human polyomaviruses to be discovered, were isolated from tissue samples in 1971 and named for the initials of the patients from which the samples were sourced (Padgett et al. 1971, Haley and Atwood 2017). Of the four human polyomaviruses that cause disease, JCPyV and BKPyV have been studied the longest, but remain enigmatic in some respects. JCPyV and BKPyV are highly prevalent in the population, with an estimated combined worldwide seroprevalence of 80% (Pinto et al. 2014). The seroprevalence of JCPyV alone is estimated to be anywhere from 40-60% (Kean et al. 2009). However, other estimates show that 60-80% of adult humans produce antibodies against JCPyV, suggesting most people may have been exposed to the virus at some point (Knowles et al. 2003). In addition, individuals are likely infected with JCPyV in childhood, with roughly 50% of the population testing seropositive beginning between the ages of 10 and 15 years (Padgett and Walker 1973). JCPyV infection likely occurs via oral-fecal route, possibly

through primary infection of the tonsils. Due to viral persistence in renal tissues, it is often excreted in urine (Assetta and Atwood 2017).

The high prevalence of JCPyV and BKPyV may be disconcerting, but their associated diseases are relatively rare. JCPyV is the only human polyomavirus known to cause disease of the nervous system (Haley and Atwood 2017). The nonpathogenic form of JCPyV is found in the kidney, and in most individuals remains there in an asymptomatic persistent infection state for life. However, if an individual becomes severely immunocompromised, the JCPyV genome can undergo rearrangement and become infectious to human glial cells (Marshall et al. 2014). If this occurs, the individual may develop Progressive Multifocal Leukoencephalopathy (PML), a fatal neurodegenerative disease (Benedetta and Atwood 2017). Interestingly, the non-rearranged ('archetype') variant of JCPyV is poorly permissible even in kidney cell lines and is not at all infectious to human glial cells. However, once rearrangement occurs both the kidney and central nervous system are found to be more permissible to viral infection (Haley and Atwood 2017). The method of viral trafficking from the kidney to the nervous system is not well understood, but several hypotheses could potentially explain the shift.

Although all patients diagnosed with PML test positive for the presence of JCPyV in brain tissues, a fair number of patients with no symptoms of PML also test positive for JCPyV in brain tissue (White et al. 1992). The presence of JCPyV in a nonpathogenic state suggests that the

virus may establish a persistent infection of the central nervous system in a very small population of individuals, like it does more commonly in the kidney. Other hypotheses suggest that the virus enters the bone marrow and undergoes rearrangement in cells expressing high levels of recombination enzymes, such as B cells (Haley and Atwood 2017). This would partially explain the restriction of JCPyV infection to glial cells in the brain, as transcription factors important for infection in glial cells are also found in B cells (Haley and Atwood 2017). As there is currently no successful animal model of JCPyV, it is immensely challenging to identify the biological route of infection of the virus. However, this may be changing as more advanced genetic techniques are used to develop mouse models (Kondo et al. 2014).

PML was first identified as a unique pathology in 1958 as a potential complication of a variety of diseases, including primarily B cell lymphoproliferative disorders (Ferenczy et al. 2012). All known PML cases at the time presented with lesions of the central nervous system accompanied by various neurological symptoms, and this paired with the presence of inclusion bodies in oligodendrocytes pointed to a viral cause (Astrom et al. 1958, Richardson EP 1961). PML remained a very rare disease until the mid 1980s, when human immunodeficiency virus (HIV) infection developed into an epidemic. PML was found to have a high incidence in acquired immunodeficiency syndrome (AIDS) patients, and currently PML affects about 3% of individuals infected with HIV (Major 2010). This information indicated a connection between PML and human

immunity; JCPyV is only known to cause disease in cases where an individual has a compromised immune system. In fact, the early 1990s brought the advent of highly active antiretroviral therapy (HAART), a treatment which improves immune system function through suppression of the HIV virus, and with it came a decline in AIDS-related PML fatalities (Haley and Atwood 2017). Unfortunately, this decline did not eliminate AIDS-related PML entirely, and PML associated with HIV infection still accounts for 80% of new PML diagnoses (Sacktor 2002). Even in the presence of HAART, the fatality rate of PML is still about 50%, which means that the need for innovations to improve treatment is dire (Assetta and Atwood 2017). It is vital to understand the mechanisms of infection so that alternative treatments can be developed, because although HAART reduces the risk of PML, it simultaneously heightens the risk of developing a fatal inflammatory reaction called immune reconstitution inflammatory syndrome, or IRIS (Steiner and Berger 2012).

Although AIDS-related PML accounts for most cases of PML, it is not the only source. With the development of immunomodulatory therapies for Multiple Sclerosis and other autoimmune disorders in the early 2000s, a new population of PML-susceptible individuals began to emerge. This group is primarily composed of individuals taking immunosuppressants like natalizumab, a monoclonal antibody designed to reduce trafficking of leukocytes into inflamed tissue (Haley and Atwood 2017). This group of patients is considerably smaller, but certain immunosuppressants (most notably natalizumab, efalizumab, rituximab and infliximab) still pose

a significant risk for development of PML, depending on the patient history and seropositivity for JCPyV (Assetta and Atwood 2017).

In the small population of individuals who develop PML, the effect is devastating. JCPyV, once activated, undergoes lytic infection of oligodendrocytes and astrocytes in the central nervous system, affecting cells which are vital for neuronal stability (Askamit et al. 1987). With infection of oligodendrocytes especially comes demyelination (loss of myelin sheath material) from neuronal axes; this leads to neuronal dysfunction and death. Because of demyelination at distinct points mainly in the white matter of the brain, physical symptoms can mirror several different diagnoses, including multiple sclerosis and stroke. Unfortunately, it is difficult to identify early stages of PML, meaning diagnosis often only occurs once symptoms are already severe. Symptoms include motor dysfunction, visual defects and speech impairment (Ferenczy et al. 2012). Diagnosis typically is done through magnetic resonance imaging (MRI) identification of viral lesions.

There is currently no specific antiviral drug against JCPyV, but use of antiretroviral drugs in HIV patients and early detection and monitoring have played a significant role in reducing PML mortality (Ferenczy et al. 2012). Numerous antiretroviral drugs have been tested for efficacy against JCPyV, but none have been successful thus far. Instead, what is considered the best option for slowing the effects of PML is restoration of the immune system, although this increases the risk of IRIS. Targeting viral spread may be another effective option, potentially through

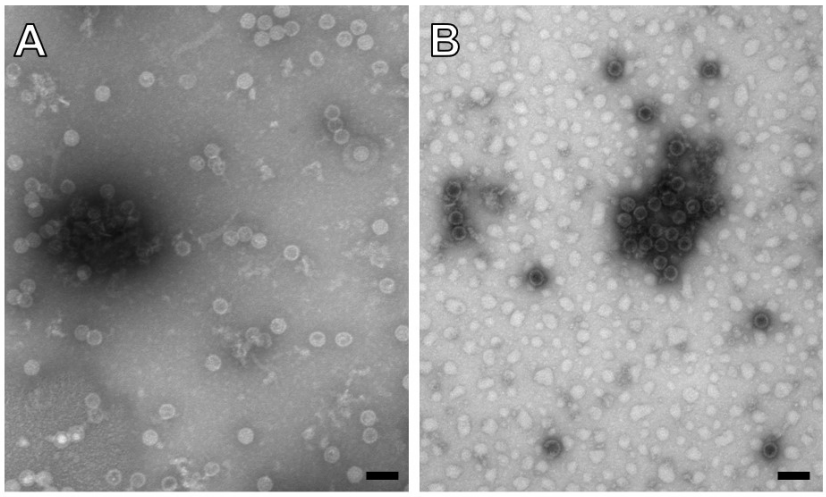

Figure 1. JC Polyomavirus and Pseudovirus
Live stained JC Polyomavirus lysate (A) and Pseudovirus (B) were both stained with uranyl acetate. Images were collected within 24 hours of staining on a Philips 410 TEM. Scale bars are 100 nm. Camera was NANOSPRT5 with 200 ms exposure time and 80.0 kV voltage. Both images are at 82000x.

inhibition of serotonin receptor subtype 2 (5-HT2R) (Pelosini et al. 2008). Overall prognosis is somewhat dictated by T cell immunocompetence, and having a cytotoxic T cell (CTL) response may indicate increased likelihood of surviving PML (Koralnik et al. 2002). Indeed, generating JCPyV antigen-specific CTLs and introducing them to a patient via adoptive transfer in conjunction with a serotonin reuptake inhibitor and another antiviral led to improvement in symptoms and clearance of JCPyV from cerebrospinal fluid (Balduzzi et al. 2011).

Surprisingly, PML is not the only disease caused by JCPyV. The virus can in rare cases lead to JC virus granule cell neuronopathy (GCN), JC virus encephalitis, JC virus meningitis and JCPyV-associated nephropathy. GCN is similar to PML in that JCPyV infects the brain, although in GCN the virus infects granule cells in the cerebellum instead of oligodendrocytes. Because the infections both occur in the CNS, the comorbidity of PML and GCN is likely high. JC virus encephalitis and meningitis are very rare, but seem to be related to the immunocompromised

state of the individual, and JCPyV-associated nephropathy is also rare, with milder symptoms than other forms of viral nephropathy (Assetta and Atwood 2017).

Viral Biology

JCPyV is a non-enveloped virus with a circular, dsDNA genome typically 5130bp in size, enclosed by an icosahedral capsid (Figure 1, Assetta and Atwood 2017). The viral capsid is composed of 72 pentamers of viral protein 1 (VP1), each bound to either a single viral protein 2 (VP2) or viral protein 3 (VP3) (Ferenczy et al. 2012). The viral genome is well characterized, and is composed of an early gene segment, a late gene segment, and separating the two, a non-coding control region (NCCR) containing the origin of replication as well as promoter and enhancer elements (Figure 2, White and Khalili 2011). The early genes are transcribed first on one strand, and produce large T antigen, small t antigen and three T antigen

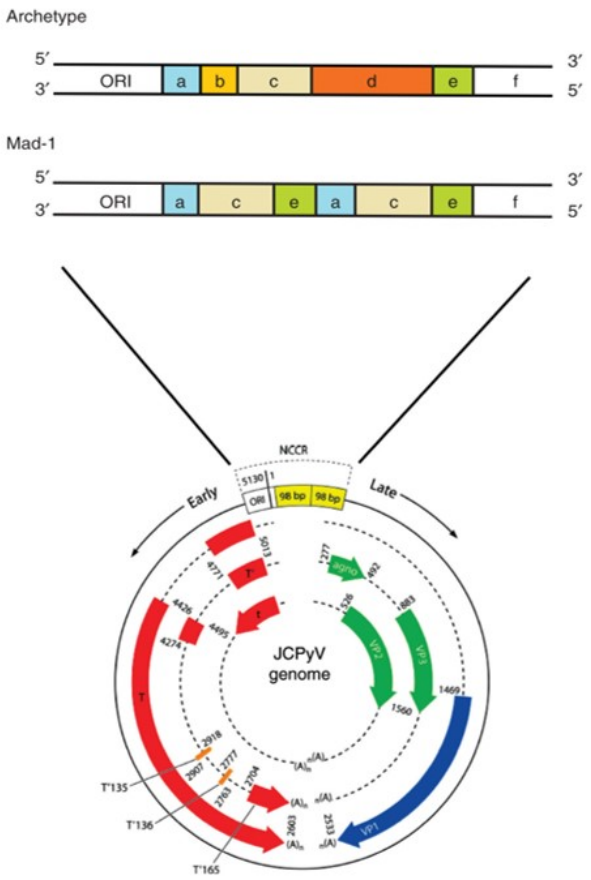

Figure 2. JC Polyomavirus Genome
Adapted from Assetta and Atwood (2017). The JCPyV genome contains both early and late gene transcription sequences, with the noncoding control region (NCCR) between the two. The NCCR can be segmented into blocks (labeled a-f in the figure) which differ between JCPyV variants. Two variants, Mad-1 and Archetype, are shown above.

splice variants. On the complementary strand, the late genes are transcribed into three structural proteins (VP1, VP2 and VP3) as well as an agnoprotein and two micro-RNAs (miRNAs) acting to downregulate large T antigen in a negative feedback loop. The NCCR defines the character of the virus in that rearrangement may lead to changes in virus infection characteristics and tissue spread. As alluded to earlier, the transmitted form of JCPyV is likely that known as ‘archetype’ JCPyV, which refers to a specific sequence in the NCCR and which is found in the kidney but rarely in the brain of PML patients. In contrast, a ‘rearranged’ NCCR carries one of several altered genetic sequences which might make it more likely to cause PML (Assetta and Atwood 2017). Like most viruses, JCPyV requires host cell machinery to replicate. JCPyV does this through the large T antigen protein, which once transcribed interacts with a series of cellular proteins to induce viral replication and assembly (Assetta and Atwood 2017).

Before the virus can co-opt host replication machinery, it must enter the cell (Figure 3). JCPyV initially binds to the target cell via α2,6-linked glycan lactoseries tetrasaccharide c (LSTc), a receptor motif which has both a necessary α2,6-linked sialic acid and a distinctive L shape (Neu et al. 2010, Assetta and Atwood 2017). JCpyV then transiently interacts with 5-hydroxytryptamine 2 receptors (5-HT2R) in an unknown mechanism, before clathrin-mediated endocytosis into the cell and subsequent trafficking into Rab-5 positive early endosomes (Pho et al. 2000, Querbes et

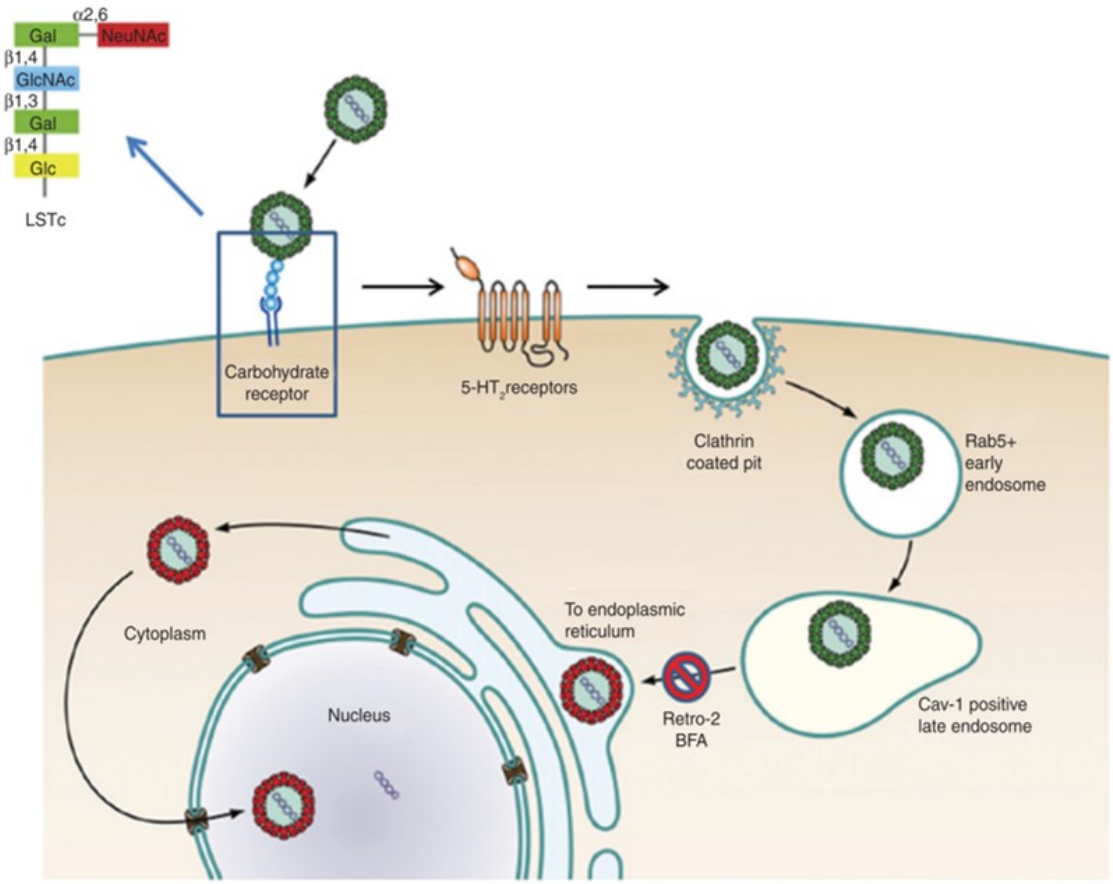

Figure 3. Infection Pathway of JCPyV
Adapted from Assetta and Atwood (2017). JCPyV binds to LSTc before 5-HT2R-facilitated clathrin-mediated entry into the cell. The virus then traffics from a Rab5+ early endosome to a Calveolin-1+ late endosome, indicating a shift between cytosolic pathways. Finally, the virus moved through the endoplasmic reticulum to the cytosol and to the nucleus for replication.

al. 2004). Next, one would expect JCPyV to traffic through Rab7-positive late endosomes, but the virus transitions to calveolin-1 positive late endosomes instead (Querbes et al. 2006). This shift in endocytic pathway could be caused by several mechanisms, including those involving 5-HT2Rs, as 5-HT2Rs are known to be endocytosed through clathrin-mediated endocytosis as well (Raote et al. 2007).

JCPyV likely uses microtubules or microfilaments to traffic through the cell to the endoplasmic reticulum (ER), where the viral capsid proceeds to degrade due to resident proteins in the ER (Assetta and Atwood 2017). The virus then uses the ER-associated degradation pathway to shuttle from the ER to the cytoplasm before entering the nucleus. Here, JCPyV finally releases its internal DNA and begins replication (Assetta and Atwood 2017).

JCPyV and Serotonin Receptors

5-HT2Rs have the potential to play a role in multiple stages of JCPyV infection, from immediately after LSTc binding to later trafficking within endosomes. 5-HT2Rs are one of seven 5-HT receptor families, each with a variety of lettered subtypes (2A, B and C, for example). There are a total of 14 5-HT receptors. Most are G-protein coupled receptors (GPCRs) except the 5-HT3A receptor, which curiously is an ion-gated channel (Raote et al. 2007, Assetta et al. 2013). GPCRs are known for having widespread effects in the cell and within body systems, and 5-HT2ARs in particular have been linked to schizophrenia, depression, anxiety, OCD and ADHD. Using a combination of immunohistochemistry and microscopy, 5-HT2AR protein was found to be expressed in all cortical layers, though most noticeably in layer 5 (Raote et al. 2007). The receptor is expressed in a variety of cell types, including astrocytes, oligodendrocytes, neurons, kidney epithelial cells and choroid plexus epithelial cells (Haley et al. 2015). The presence of 5-HT2R on so many cell types does not indicate viral permissivity; it is more likely that 5-HT2R are used after

JCPyV has already bound to an LSTc motif.

JCPyV uses the three subtypes of 5-HT2R (5-HT2AR, 5-HT2BR and 5-HT2CR) to infect cells, and these three receptors may fulfill complementary roles (Elphick et al. 2004, Maginnis et al. 2010, Assetta et al. 2013). Elphick et al. (2004) showed that inhibition of 5-HT2ARs using antagonists or function-blocking antibodies also inhibited JCPyV infection, but not infection of a control virus (SV40). In addition, transfection of a human embryonic kidney cell line with little expression of 5-HT2ARs with the receptor rescued infection levels of JCPyV. Lastly, use of antibodies directed against the N-terminus of the 5-HT2AR indicated potential colocalization between the receptor and the virus in endosomal compartments. Together, this data indicates the importance of 5-HT2ARs in JCPyV infection, but not the specific mechanisms by which the virus utilizes the receptors. Assetta et al. (2013) went on to confirm that the effect on JCPyV was specific to 5-HT2Rs, and not just 5-HT2ARs; all three subtypes of 5-HT2R are involved in JCPyV infection. When upregulation of 5-HT2Rs was induced, JCPyV binding to the cell surface remained unchanged, suggesting that interaction with the 5-HT2R occurs independently and after virus binding to LSTc (Assetta et al. 2013).

Continuing along this thread, Assetta et al. (2019) used a proximity-ligation assay (PLA) to evaluate molecular interaction between JCPyV and 5-HT2ARs. Interaction was seen for all members of the 5-HT2R family, and subsequent CRISPR-Cas9 knockouts of the proteins show

that removal of the second intracellular loop of the receptor inhibits infection. This loop is likely important for receptor internalization through interaction with β-arrestin (Assetta et al. 2019). 5-HT2Rs are known to heterodimerize with other proteins such as the metabotropic glutamatergic receptor 2 ($mGlu_2$), but little work has been done thus far on dimerization interactions between 5-HT2AR, 5-HT2BR and 5-HT2CR (Lukasiewicz et al. 2018, Raote et al. 2007). Understanding these interactions, especially because it is unclear what type of interaction JCPyV has with the receptors, will provide a significantly greater understanding of the mechanism of cell entry of JCPyV.

Several methods of evaluating dimerization have been described, with particular attention given to the specificity of proximity ligation assay (Faron-Gorecka et al. 2019). However, this method is less effective when evaluating receptor location in relation to structures not directly involved in the proximity ligation reaction. Immunohistochemistry has been used against 5-HT2Rs with varying success, but for the level of resolution desired in evaluating the subcellular location of 5-HT2R, antibodies directed against the 5-HT2R protein subtypes (2A, 2B and 2C) are not specific enough to warrant accurate data (Raote et al. 2007, unpublished Atwood lab results). One solution which would allow precise characterization of 5-HT2R location at the subcellular level is protein tagging of the receptor itself. In this study, 5-HT2Rs were stably modified with unique fluorescent proteins amended to the C-terminus of each 5-HT2R subtype. These modified

genes were inserted into inducible, selectable plasmids before being integrated into various cell lines using a lentiviral vector. 5-HT2R protein expression was evaluated before the cell lines were challenged with JCPyV or control virus. Confocal microscopy was used to evaluate colocalization of receptors in both normal and JCPyV-infection states. Understanding the types of interactions between 5-HT2Rs during viral infection highlights the role of these receptors in JCPyV infection and leads to potential exploration into new avenues for treatment or prevention of PML.

Methods

Construct Design

Initial plasmid backbone was found on Addgene and selected based on tetracycline-ON inducibility, lentiviral compatibility and inclusion of common genes for drug resistance (ampicillin and puromycin). The selected plasmid, pLIX_403, was a gift from David Root (Addgene # 41395; http://n2t.net/addgene:41395; RRID: Addgene_41395). The construct included a TRE promoter and a gateway cloning insert. Original pLIX_403 is 9396bp, including gateway sequence. To modify plasmid into NEBuilder®-compatible sequence, primers sourced from Integrated DNA Technologies (IDT) (www.idtdna.com) were ordered specific to each desired 5-HT2R insert. Primers were designed using NEBuilder® protocol (https://www.neb.com/) and can be found in the Supplemental Information section under “Gateway Modified Primers.” 5-HT receptor insert genes were sourced from NCBI (https://www.ncbi.nlm.nih.gov/gene) and cross-checked using NCBI BLAST. The human 5-HT2AR sequence was found under “Homo sapiens 5-hydroxytryptamine receptor 2A (HTR2A), transcript variant 1, mRNA full sequence,” the human 5-HT2BR sequence was found under “Homo sapiens 5-hydroxytryptamine receptor 2B (HTR2B), transcript variant 1, mRNA full sequence,” and the human 5-HT2CR sequence was found under “Homo sapiens 5-hydroxytryptamine receptor 2C (HTR2C), transcript variant 1, mRNA.” Fluorescent proteins were selected based on expression characteristics and minimal wavelength

overlap. Fluorescent protein sequences were found on the Addgene website. The three fluorophores selected were mAzurite-N1 (EBFP), mCherry2-N1 (mCherry) and mEGFP-1 (EGFP). All fluorescent proteins were monomers to reduce the risk of hairpin formation or dimerization, and were cross-checked on NCBI BLAST to ensure they were designed for mammalian (human) expression.

DNA Extraction

DNA was extracted from bacteria using either a QIAGEN® Plasmid Mini or Maxi Kit. Kits were ordered online from QIAGEN.® Protocol was followed as detailed in product manual; the general procedure is a series of centrifugation and wash steps, with Miniprep kit detailed broadly as followed. LB broth containing expanded bacteria was spun down via centrifuge and resuspended in buffer, then a lysis buffer was added in proportional volume. Cells were allowed to lyse and release plasmid DNA, then solution was neutralized and non-protein molecules precipitated out of solution. This was centrifuged and the resulting supernatant applied to a spin column. The spin column was washed with several buffers and then DNA eluted into a microcentrifuge tube.

DNA Quantification

DNA was quantified with a Thermofisher Scientific Nanodrop™ spectrophotometer. If results suggested a concentration below approximately 100ng/µl, DNA was additionally quantified using a Qbit DNA quantification assay on a Qbit 3.0 Fluorometer from Thermofisher Scientific. This

provided a more accurate count of DNA concentration based on the use of two prepared standards.

Gel Electrophoresis

1% Agarose gels were prepared by dissolution of 1 g Agarose powder in 100 mL 1X TAE buffer. Solution was heated in a microwave in bursts for 90 seconds until completely in solution. The flask containing the solution was then swirled and 5 µL of Ethidium Bromide was added to solution and swirled again to mix. This was poured into a gel mold and left to cool with inserted comb for 25 minutes. The comb was removed and gel chamber filled with 1X TAE buffer to just above the gel surface. Samples were mixed 1:1 with 2X loading dye and an appropriate ladder (either 100bp or 1 kilobase) selected. Samples were loaded and electrical current applied at a steady voltage for 30 minutes to 1.5 hours. Completed gels were read and imaged using a UV light digital gel imaging chamber.

Gateway Modification

Gateway modified primers were used to generate appropriate overhangs and remove gateway sequence from pLIX_403 using polymerase chain reaction (PCR). pLIX_403 bacterial agar stab was used to expand bacteria containing the plasmid in LB broth with ampicillin at 1:1000 concentration, to select for pLIX_403-positive colonies. Bacteria were grown for 12 hours in 5 mL of broth, then spread over an ampicillin-positive agarose plate and incubated at 37C for 24 hours.

A single colony was selected from the resulting plate and expanded once more in 8 mL of LB broth with added ampicillin, to ensure homogeneity of resulting bacteria. The pLIX_403 plasmid was isolated from the bacteria using a MiniPrep kit, detailed in “DNA Expansion” methods section. Resulting DNA was quantified with Qbit Assay, detailed in “DNA Quantification” methods section. Approximately 90ng of DNA was used for PCR. Program was run for 30 seconds at 98C, then through 25 cycles of the sequence: 98C for 10 seconds, 64C for 30 seconds, and 72C for 8 minutes. Annealing step length was determined based on backbone length (30 seconds per plasmid kilobase, with additional time resultant of troubleshooting). A final annealing step was added after cycling (72C for 12 minutes) and samples were held at 4C indefinitely post-reaction. Gel electrophoresis was used to confirm that DNA products of the correct size were generated in the reaction (see “Gel Electrophoresis” methods section).

NEBuilder® Reaction

The NEBuilder Kit was used for DNA cloning (see references for manual), due to its ability to anneal fragments quickly and seamlessly. To generate primers for NEBuilder reaction, insert sequences were aligned with the corresponding gateway-negative plasmid vector. Overlaps between vector and insert were balanced with each about half of the total primer sequence. Primers were used in Gateway Modification step to generate appropriate overhangs for reaction (see methods section, “Gateway Modification”). Between 100 and 200 ng of insert DNA was used

in each reaction, based on troubleshooting and initial insert concentration. The reaction was set up on ice, and included insert DNA (with the linked 5-HT receptor and fluorescent protein genes), pLIX_403 gateway-negative vector with appropriate overhangs, NEBuilder DNA HiFi Assembly Master Mix, and deionized water. Samples were incubated at 50C for 15 minutes, then the product transferred back to ice. Next, XL-10 GOLD recombinase-free bacteria were used for bacterial transformation. Bacteria were thawed on ice and 2 µL of assembled NEBuilder product added to each tube. Bacteria were gently mixed and incubated on ice for 30 minutes, before heat shock at 42C for 30 seconds. Transformed bacteria were then placed back on ice for 2 minutes and then 950 µL room-temperature SOC media added to each tube. Tubes were incubated at 37C for 60 minutes, with 200rpm horizontal shaking. Ampicillin-positive agarose gel plates were heated to 37C, and 100 µL of bacterial broth spread evenly across each plate. Plates were incubated at 37C for 24-48 hours, and bacteria evaluated for plasmid sequence viability.

Sanger Sequencing and Plasmid Validation

Because plasmids could contain recombination edits altering the initial sequence, gel electrophoresis was used to identify the presence of 5-HT receptor insert, and the final sequence confirmation was validated through direct Sanger Sequencing. NEBuilder product-transformed bacterial colonies were expanded and DNA extracted through QIAGEN® Miniprep (see methods section, “DNA Extraction”). DNA was then processed through PCR with primers designed to

identify the overlap region between the plasmid vector and insert. Primers for each insert can be seen in the Supplemental Information, under “Validation Primers.” Primers were also used in Sanger Sequencing, ordered through Genewiz, Inc. For sequencing, forward and reverse primers were added to the sample DNA individually. If appropriately modified bacterial colonies could not be identified in the first round of screening, an adapted protocol was used to streamline PCR analysis. In this adapted protocol, instead of Miniprep DNA extraction, 1 µL of bacterial colony (diluted in distilled water) was added directly to the PCR reaction in place of DNA. The sample was then heated to 94C for 5 min prior to PCR reaction to degrade bacterial membranes.

Cell Cultures

Immortalized Human Embryonic Kidney (HEK 293A) cells were used for initial transfections due to relative transfectability. Immortalized Human Fetal Glial (SVGA) cells were used in additional transfections and stable transductions due to virus permissivity. A knockout SVGA cell line generated using CRISPR-Cas9 by Dr. Benedetta Assetta (SVG-2ABCKO) was used for final experimentation, as these cells are both permissive to JCPyV and contain no endogenous 5-HT2Rs (Assetta et al. 2019). Cells were cultured in non-pyrogenic plastic flasks, using either Mimimum Essential Media, MEM (for SVGA and SVG-2ABCKO cells) or Dulbecco’s Modified Essential Media, DMEM (for HEK 293A cells) with 10% fetal bovine serum (FBS) and 1% Antibiotic-antimycotic. Cells were age-matched and were passaged weekly in a biohazard hood.

Transfections

Transient transfections of modified plasmids into cell lines were done using Lipofectamine™ 3000 Reagent, sourced from ThermoFisher Scientific. Cells were removed from adherent surface and suspended in solution, then quantified using a Countess™ Cell Counter. Cells were plated in 24-well plates at a concentration predicting 75% confluency at the time of transfection. To transfect DNA into cells, lipofectamine was diluted in Opti-MEM™ Medium with 1.5 µL lipofectamine per 50 µL Opti-MEM (about 1.5 µL/mL lipofectamine as a final concentration). Separately, DNA was diluted in Opti-MEM and P3000™ reagent added, then this solution was added in a 1:1 ratio to the lipofectamine solution. Samples were incubated at room temperature for 15 minutes then added to 24-well plate with final DNA concentration at about 300 ng/mL and left for 6-12 hours. Cell media was changed after 12 hours to reduce toxicity and prevent cell death, then doxycycline added at 1 µg/mL. Doxycycline Hyclate was sourced from Selleckchem and the powdered drug was suspended in DMSO. Cells were incubated for 24-48 hours and then imaged or fixed.

Fixation and Staining

Cells were fixed in 4% PFA (for SVGA and SVG-2ABCKO cells) or 100% ice-cold methanol (for HEK 293A cells) for initial transfections and VP1 staining. Media was aspirated and rinsed with 1X PBS, then replaced with 0.5 mL 4% PFA. Plates were incubated at room temperature for 20 minutes, then PFA was removed (under chemical fume hood) and sample was carefully rinsed

with PBS three times. If methanol was used, 0.5 mL of ice-cold 100% methanol was added to cells on ice and incubated at room temperature for 20 minutes before removal under fume hood. For T-antigen staining, cells were fixed in ice-cold 100% ethanol. For this procedure, PBS was aspirated from live cells and 0.5 mL 100% ethanol (on ice) was added. Cells were incubated for 20 minutes at room temperature, then ethanol was removed (under chemical fume hood). Variation in fixation technique depended on prior troubleshooting by the Atwood laboratory. For staining with DAPI, a nuclear marker, DAPI diluted 1:1000 in 1X PBS was added (300 µL per well in a 24-well plate) to cells. Sample was incubated in the dark at room temperature for 10 minutes, then rinsed 3 times with 1X PBS and stored at 4C. For Red Nuclear Mask staining, the same procedure was used except the stain was diluted at 1:500 and samples were incubated for 25-30 minutes. For immunostaining against VP1, cells were fixed and in PBS. The PBS was aspirated and replaced with 1 mL of 1% Triton-X, a membrane permeabilizer. Cells were blocked with goat serum for 30 minutes and then switched to primary antibody for 2 hours at 37C (anti-VP1, pAb 597) at 1:50 dilution from stock. Secondary antibody (AlexaFluor goat anti-mouse 488 or AlexaFluor goat anti-mouse 594) was used at a 1:500 dilution from stock and incubated at 37C with cells for 1 hour. Next, cells were washed and stained with DAPI if necessary. In staining for T-antigen, methodology was similar to that for VP1 immunochemistry. Primary antibody (anti-T-antigen) was used at a 1:1 dilution from stock. To ensure cell adhesion, plates were coated with

Poly-L-Lysine for 1 hour prior to plating. Poly-L-Lysine was washed thoroughly from plates with distilled water after coating. Coverslips were #1.5 and were mounted on glass slides in fluorescence mounting media before being sealed with nail polish.

Addition of Ligands to Cell Cultures and Viral Infection

Several experiments were done which involved addition of ligand to a cell culture which had been transfected or transduced with modified 5-HT2Rs. 5-HT was used at 10 mM in DMSO. Modified prepared JCPyV which had been linked to a fluorophore with emission at 405 nm or 633 nm was used at a 1:30 dilution from stock. Unpurified JCPyV was used at 1:20 in HEK cells and 1:100 in SVGA and SVG-2ABCKO cells due to their respective permissivity to virus. SV40 virus was used at a 1:50 dilution from stock. In one representative experiment, SVGA cells were serum-starved for 24 hours prior to addition of ligand, to force cell cycle synchronization and to bring receptor expression to basal levels. Ligand was added for varied time points before cell fixation and storage in 1X PBS at 20C. In experiments requiring ligand binding (virus or 5-HT) at specific time points, cells were incubated on ice for 20 minutes to cool membranes. Ligand was added to respective cells and incubated for 1 hour on ice to allow binding without membrane entry. At this time, ligand solution was removed and replaced with room temperature media, before being shifted to 37C for specified time frame. After post-binding time point, cells were immediately fixed in 4% PFA. For JCPyV infection of transfected HEK 293A cells with the goal of viral protein expression evaluation,

cells were grown to be 70-90% confluent in a well plate in the presence of doxycycline. Virus lysate was used at 1:20 dilution from stock and added to cells in serum free media. Cells were incubated at 37C for 2 hours, with periodic perturbance to ensure viral spread. After 2 hours, complete media was added to virus solution and cells incubated at 37C for five days before fixation in ethanol and staining. For JCPyV infection of SVGA cells, the above procedure was used with JCPyV at 1:100 and incubation for three instead of five days as the only modifications.

Lentivirus Generation and Stable Transduction

Lenti-X 293T cells (sourced from ClonTech) were grown in 75 cm^2 plastic flasks to 70% confluency in DMEM with 10% FBS and no antibiotic. Lenti-X cells were transfected with a packaging plasmid (pCMV-dr8.91), an envelope plasmid (VSV-G) and the desired DNA plasmid (one of the three modified 5-HT2Rs). pLKO.1 GFP plasmid was used as a positive control vector and the original pLIX_403 plasmid was used as an experimental control vector. DNA was diluted in serum-free (FBS-free) media. Transfection was done using FuGENE® Transfection Reagent (sourced from Promega). FuGENE® was diluted in serum-free media and incubated for 5 minutes at room temperature. DNA plasmid mix was added to FuGENE® in a dropwise manner, with minimal shaking. Solution was incubated an additional 20 minutes at room temperature, then added to Lenti-X cells dropwise. FuGENE® was retained in cell media for 18 hours. Media was switched to 30% FBS with 1% antibiotic-antimycotic, and left for 8-12 hours to induce initial virus production.

This was then harvested and filtered through a 45 μm filter tip, and fresh media replaced to keep the cells alive. The replaced media was harvested, filtered and replaced twice more with 8-12 hour consecutive incubation periods, and collected into a 50 mL conical vial. Polybrene was added to final lentivirus solution at 8 μg/mL. To transduce target cell line with virus, cells were grown in 10% FBS media with 1% antibiotic-antimycotic until 75% confluent. Media was then replaced with 10 mL of lentivirus supernatant and cells kept at 37C for 8-12 hours. The lentivirus supernatant was then removed and replaced with fresh supernatant for a new infection. This was repeated once 12-16 hours after the second infection, and cells kept at 37C for 8-12 hours. Cells were then switched to media with 15% FBS and puromycin, a selection drug, added at 1 μg/mL. Cells were allowed to grow for several days in selection media before sorting.

Flow-Activated Cell Sorting (FACS)

Cells in solution were diluted to a concentration close to 10^8 cells/mL. Using glass 12x75 mm flow tubes chilled on ice, cells were transferred to the Sidney E. Frank Flow Cytometry and Sorting Facility FACS machine. Cells were gated for fluorescent-positive samples and sorted cells were expanded in the presence of antibiotic-antimycotic in 25 cm^2 plastic flasks.

gRNA Site-Directed Mutagenesis

SVG-2ABCKO cell line required base-pair modification to prevent residual CRISPR-Cas9 gRNA targeting of the modified 5-HT2R plasmids. New England Biolabs Q5® Site-Directed Mutagenesis

Kit was used to modify each of the three plasmids. Primers can be found in Supplemental Information under “Site-Directed Mutagenesis Primers.” Primers were designed to modify existing gRNA sequence with silent mutations. Kit directions were followed and samples modified through PCR and subsequent expansion through transformed DH5Alpha bacteria. Resulting bacterial colonies were screened for appropriate modifications using Sanger Sequencing through GENEWIZ.®

Electron Microscopy (EM) Preparation

EM sample grids were placed under UV light for 20 minutes. JCPyV lysate and pseudovirus (gifts from Jenna Morris-Love) were added to grids and incubated for 5 minutes at room temperature. Uranyl acetate was filtered through a 0.22 µm filter tip before being dripped onto a clean and protected parafilm sheet. Grids were placed facedown on uranyl acetate droplets and allowed to stain for 1 minute. Grids were then dried and transported to the Philips 410 Transmission Electron Microscope (TEM) located in Sidney E. Frank Hall at Brown University for imaging.

Storage of Bacteria

All bacterial plasmids were saved at -80C as glycerol stocks, made with 500 µL of 50% Glycerol and 500 µL of bacteria in LB broth. Bacterial stocks were placed directly in -80C freezer and kept indefinitely.

Storage of Mammalian Cell Lines

Modified cell lines were placed in indefinite storage at -80C. A 75 cm^2 flask of 90% confluent cells was resuspended in a solution of 70% media, 20% fetal bovine serum (FBS) and 10% DMSO. This solution was aliquoted into three cyrogenic tubes and placed in a box containing an isopropanol bath for slow freezing down to -80C. Cells were transferred to storage in liquid nitrogen after 24 hours.

Image Analysis

Samples were imaged using either fluorescent microscopy or confocal microscopy (excepting TEM images). Live cell imaging was done using the ZOE™ Fluorescent Cell Imager from Bio-Rad. Fluorescent microscopy was done using a Nikon Ti2-E Fluorescence Microscope. Confocal microscopy was done using a Zeiss LSM 710 Confocal Laser Scanning Microscope. All images were taken in the Atwood Laboratory or the 70 Ship Street Facilities Core run by the Leduc Bioimaging Facility at Brown University.

Results

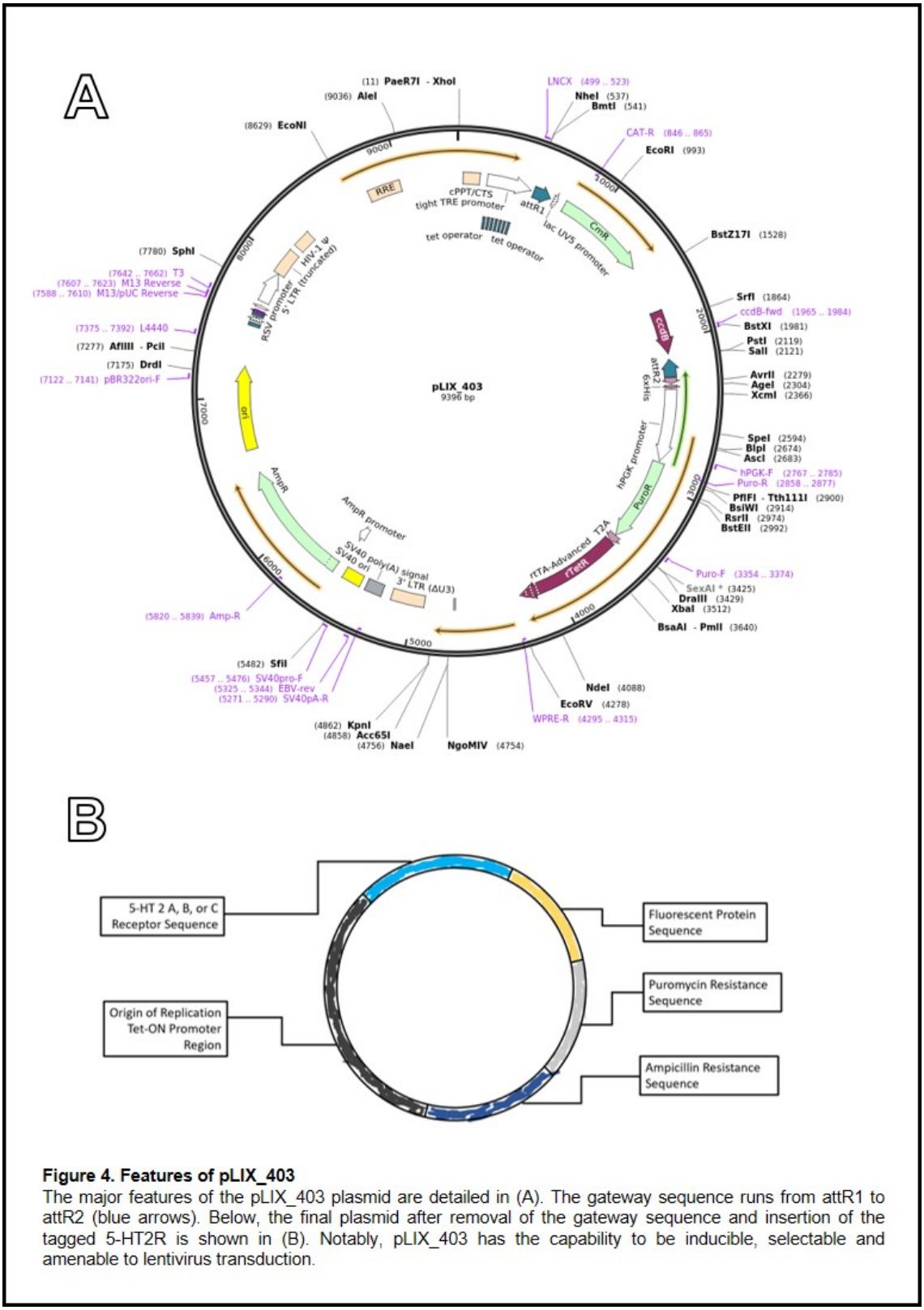

Figure 4. Features of pLIX_403
The major features of the pLIX_403 plasmid are detailed in (A). The gateway sequence runs from attR1 to attR2 (blue arrows). Below, the final plasmid after removal of the gateway sequence and insertion of the tagged 5-HT2R is shown in (B). Notably, pLIX_403 has the capability to be inducible, selectable and amenable to lentivirus transduction.

Generation of modified 5-HT2R Plasmids

In order to build a plasmid containing the desired features, several possible vector backbones were examined for efficiency and viability. pLIX_403 was selected as the optimal plasmid due to several characteristics (Figure 4). It was relatively small in size, which may improve the efficiency of transcription in the cell. It contained elements necessary for lentiviral integration and transduction into competent cells, and it contained selection genes for both prokaryotic and eukaryotic expression (ampicillin and puromycin, respectively). pLIX_403 also contained a Tet-Responsive Element promoter sequence, making it ideal for experiments requiring temporary expression of the genes of interest. pLIX_403 is designed to be Tet-ON inducible, meaning the plasmid DNA is transcribed only in the presence of doxycycline, a common tetracycline derivative (Figure 5).

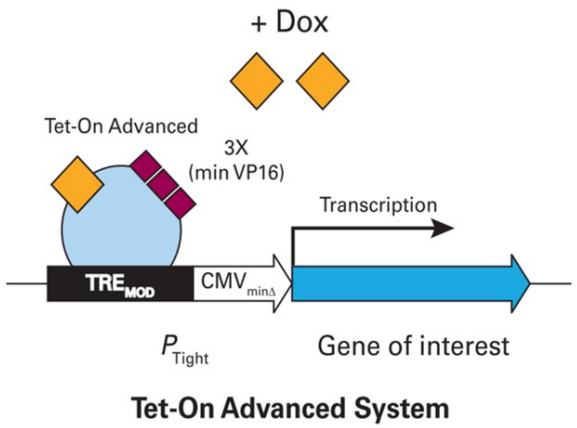

Figure 5. Tetracycline-ON Inducible Systems
In the presence of doxycycline (DOX), the transactivator protein (Tet-On Advanced) binds to the Tet-Responsive Element (TRE) within the inducible promoter (P). This paired to a CMV promoter results in transcription of the desired gene elements. Figure adapted from ClonTech Protocol No. PT3898–1 (see references).

Because the plasmid also contained Gateway cloning-compatible attR sites, a cloning methodology had to be selected to be most efficient and with least risk of error. Three serotonin receptors were selected for modification based on previous experiments: 5-HT2A, 5-HT2B and

5-HT2C receptors (Assetta et al. 2013). These would be linked at the C-terminal (intracellular) end of the protein to three unique fluorescent protein sequences, resulting in three stably tagged receptors. However, these sequences were ordered as linear DNA and were not Gateway cloning compatible. The New England BioLabs (NEBuilder®) DNA Assembly Kit was identified as an efficient way to insert linear DNA sequences into a plasmid after removal of the gateway sequence. This method was selected over insertion of the modified 5-HT2 receptor sequences into gateway-compatible plasmids.

Three fluorescent proteins were designated for linking to the three 5-HT2 receptors. Enhanced green fluorescent protein (EGFP) was selected due to its bright and highly photostable expression. In its monomeric form, EGFP has peak excitation at a 490 nm wavelength and peak emission at a 509 nm wavelength of light. mCherry was selected as a monomeric protein with strong and stable fluorescence, and had peak excitation at 587 nm and emission at 610 nm. Lastly, a monomeric form of enhanced blue fluorescent protein (EBFP) was chosen as the third protein to minimize spectral overlap. EBFP has a peak excitation at 386 nm and peak emission at 448 nm. This means that the confocal and fluorescence microscopes would be compatible with these proteins with minimal fluorescence bleed-through between channels. The LSM 710 confocal microscope has laser lines at 405 nm, 488 nm and 564 nm which is ideal for excitation of EBFP, EGFP and mCherry, respectively. Fluorescence microscopes were used with DAPI, FITC and

TRITC filters for imaging EBFP, EGFP and mCherry, respectively.

When generating linear insert sequences, stop codons were removed from the end of each 5-HT receptor sequence. The 5-HT2AR insert was designed to utilize the His tag, a short sequence of six histidine residues, found in the gateway sequence. During the NEBuilder® reaction, primers were used at sites which conserved this tag. In the 5-HT2BR and 5-HT2CR, this tag was removed during PCR. Ideally, the presence of the tag could be used biochemically to partially differentiate receptors if needed.

The gateway cloning-compatible pLIX_403 plasmid was received in a bacterial colony and expanded in LB broth under selection from ampicillin (100 µg/mL) before being spread on ampicillin-positive agarose gel plates overnight at 37C. A single colony was selected from the plate and expanded for 16 hours in ampicillin, which ensured that the resulting bacteria contained homogenous genomes. Plasmid DNA was prepared using Maxiprep kit, and its concentration evaluated using Nanodrop Spectrophotometry. Primers were ordered for PCR amplification and linearization of the plasmid with overlaps specific for each of the three 5-HT2 receptor inserts (see Supplemental Information, “Gateway Modified Primers”). A general PCR protocol was adapted to prioritize Tm temperatures for each primer pair. A final annealing temperature of 64C was selected with a prolonged extension time to ensure proper product formation was used for generating insert-specific linearized plasmids (Figure 6).

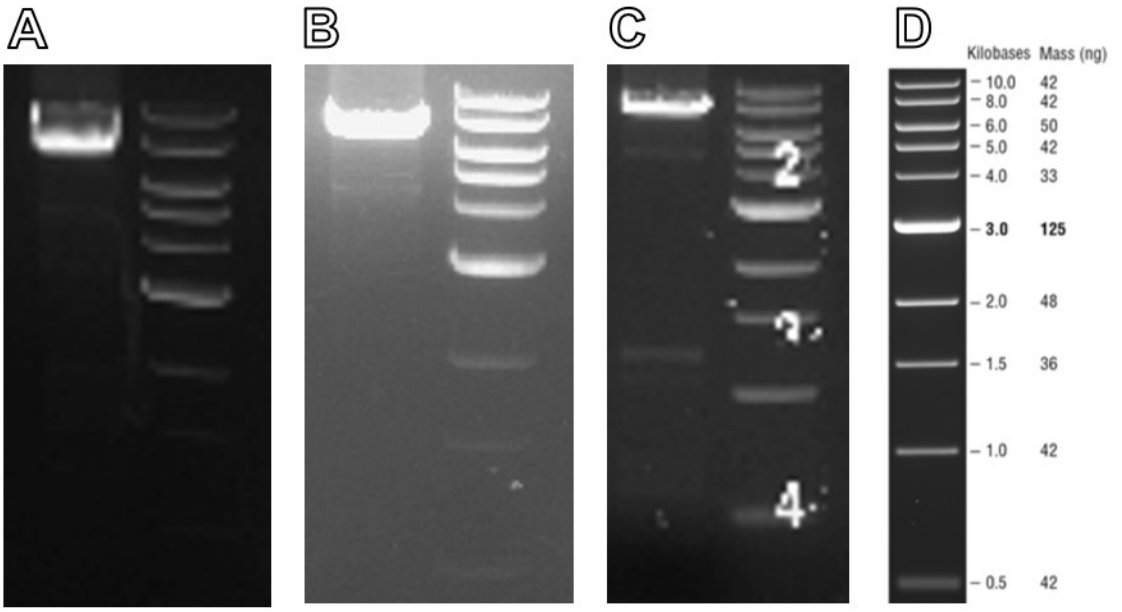

Figure 6. Plasmid Linearization
Removal of the Gateway sequence was done through PCR amplification of non-Gateway DNA (primers can be found in Supplemental Information, "Gateway Modified Primers"). The resulting linearized sequence would have blunted ends with an overlap matching the ends of the fluorescent 5-HT2R sequence. The linearized target sequence length is 7,628 bp for all three inserts. Successful DNA linearization reactions were identified via gel electrophoresis and are shown in the left lane of each panel for 5-HT2AR+EBFP (A), 5-HT2BR+mCherry (B) and 5-HT2CR+EGFP (C). A minimum of 30 ng pLIX_403 DNA was used per lane. Gels were run at 110 V for about 1 hour before visualization. A 1 Kb ladder reference is shown in (D), image is sourced from New England Biolabs, www.neb.com.

Products were identified at the correct size for plasmids specific for 5-HT2AR+EBFP (Figure 6A), 5-HT2BR+mCherry (Figure 6B) and 5-HT2CR+EGFP (Figure 6C). The expected products were 7.628 Kb in size for all three plasmids. Interestingly, additional DNA products can be seen in the completed gel, particularly in Figure 6C where there are bands at approximately 1.3 Kb and 5 Kb in addition to the expected product at 7.6 Kb. This was seen consistently and may be a result of aspecific priming during PCR. However, off-target products were at a low enough concentration (based on the low intensity of the band, where intensity has a direct

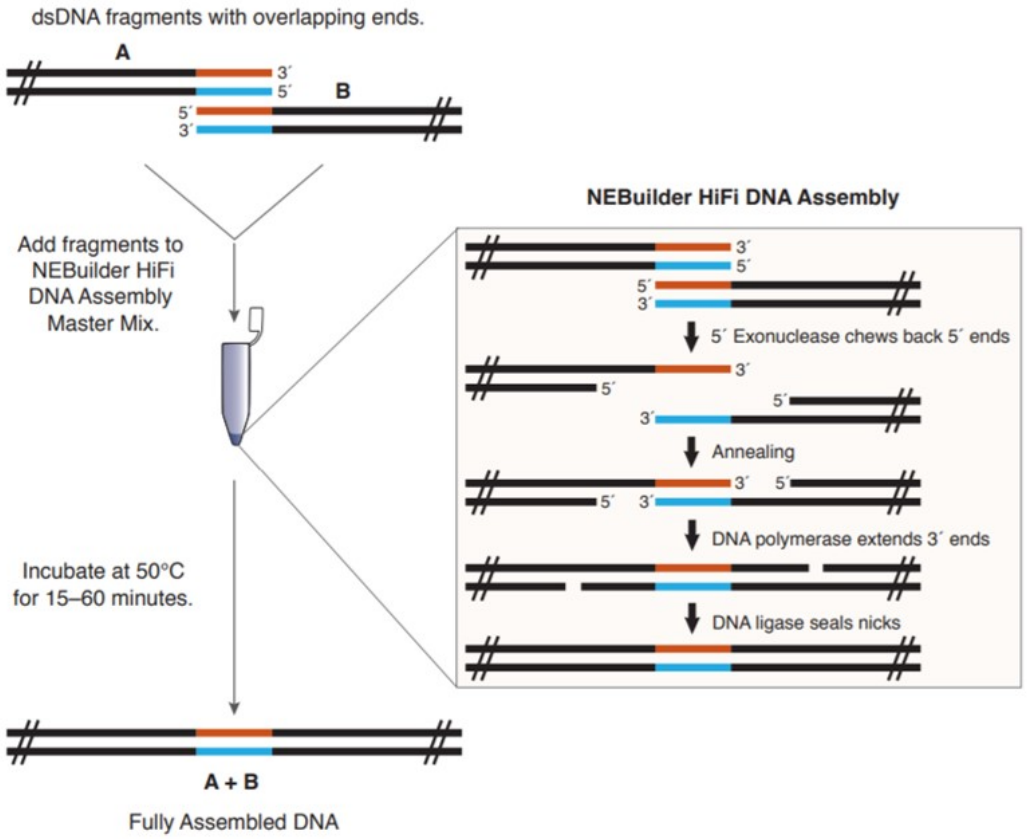

Figure 7. Overview of NEBuilder HiFi DNA Assembly Method
DNA fragments are designed with an overlap between two blunt end segments of the fragment DNA. This is combined with reaction mix, which sequentially removes fragment 5' ends, anneals the overhangs, and completes the dsDNA sequence. This reaction is fast (15 minutes), can be done with multiple fragments, and has high fidelity. Figure adapted from NEBuilder User Protocol (see References).

correlation to ethidium bromide binding to DNA) to proceed with the NEBuilder® Reaction, so time was not spent troubleshooting.

Linearized plasmids could then be re-circularized during ligation to modified 5-HT2R insert. Figure 7 describes the general schema of the NEBuilder® reaction. The linearized plasmid acts as the vector backbone, with blunted ends containing a priming sequence which overlaps with the priming sequence of the 5-HT2R insert ends. During the reaction, the 5' ends of both

pieces are eaten away by an exonuclease, leaving only the 3' overlaps. Because these sequences are complementary, and the reaction is done at an appropriate temperature for annealing, the overhangs between the vector and insert align with high specificity. Missing nucleotides are then replaced via DNA polymerase, and DNA ligase seals the strands, producing an un-nicked, re-circularized plasmid containing the gene of interest.

After the reaction, products were transformed into XL-10 GOLD bacteria, which are known to be recombinase-free. This bacterial strain was selected after products transformed into puc19 bacteria (recommended by NEB) resulted in apparent recombination events. Next, ampicillin-resistant bacteria (meaning they were presumably pLIX_403-positive) were screened for the appropriate insert by PCR. A similar protocol was used as previously, with a shorter extension time and fewer cycles. Initially, all transformed colonies were screened by Miniprep and subsequent quantification and PCR of bacterial DNA. Because this was time consuming and complicated the troubleshooting process, direct addition of water-suspended bacteria to the PCR was attempted. Prior to starting the PCR, the samples were held at 94C for 5 minutes to break down bacterial membranes and denature proteins. This approach was successful, and insert-specific primers (in Supplemental Information, "Validation Primers") were used with PCR to amplify a ~500 bp segment of both vector and modified 5-HT2R to ensure proper insertion (Figure 8).

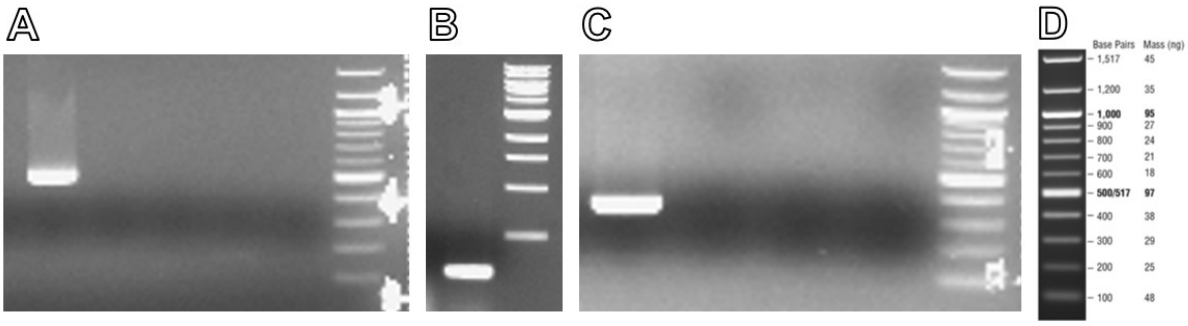

Figure 8. NEB® Reaction and 5-HT2R Insert Confirmation
The NEBuilder® reaction was used to ligate 5-HT2AR+EBFP, 5-HT2BR+mCherry, or 5-HT2CR+EGFP to the appropriate linearized pLIX_403 plasmid. Successful reactions were identified via gel electrophoresis and are shown in the left lane of each panel for 5-HT2AR+EBFP (A), 5-HT2BR+mCherry (B) and 5-HT2CR+EGFP (C). DNA samples were sourced from direct bacterial colonies (see methods, "Sanger Sequencing and Plasmid Validation"). The primers (see Supplemental Information, "Validation Primers") targeted overlap between the plasmid backbone and the inserted serotonin sequence to produce a product with size 543 bp for 5-HT2AR+BFP, 596 bp for 5-HT2BR+mCherry and 523 bp for 5-HT2CR+EGFP. Gels were run at 90 V for 40-50 minutes before visualization. A 100 bp ladder reference is shown in (D), sourced from New England Biolabs, www.neb.com. Panel (B) was run with a 1 Kb ladder (reference Figure 6).

Figure 8A, showing a successful amplification of the modified 5-HT2AR+EBFP plasmid, and 8C, showing successful amplification of modified 5-HT2CR+EGFP, are both run alongside a 100 bp ladder, with a reference in 8D. Figure 8B, showing successful amplification of the modified 5-HT2BR+mCherry plasmid, was run alongside a 1 Kb ladder but approximately falls where expected (See Figure 6D for 1 Kb ladder reference). The modified 5-HT2AR+EBFP product was expected to be 523 bp in size, the 5-HT2BR+mCherry product was expected to be 596 bp in size, and the 5-HT2CR+EGFP product was expected to be 543 bp in size. Gels were all run at 90 V for about 40 minutes, but slight differences in run time account for differences in ladder length. Bacterial colonies with successful amplification of the overlap region were marked and expanded, then their DNA extracted via Miniprep.

Transient Transfection of Labeled 5-HT2Rs and Evaluation of Expression Morphology

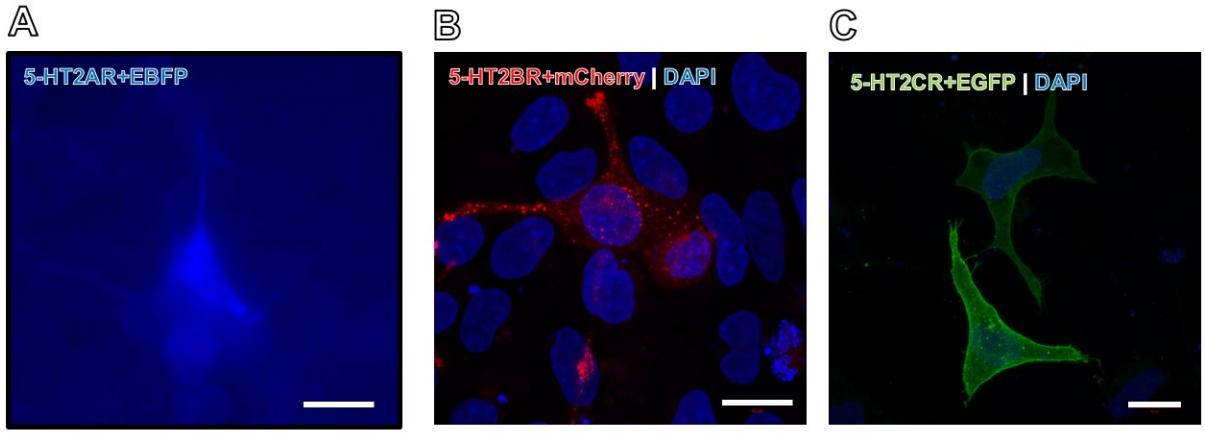

Figure 9. Transient Transfection of HEK 293A with Modified 5-HT2Rs
HEK 293A cells were transiently transfected using lipofectamine and induced with doxycycline for 48 hours. In (A), the resulting 5-HT2AR+EBFP-modified cells were imaged live on a fluorescent microscope. Cells modified with 5-HT2BR+mCherry (B), and cells modified with 5-HT2CR+EGFP (C) were both fixed and stained with DAPI before confocal imaging. Membrane expression of the receptor can be seen in (A) and (C). Scale bars are set at 20 μm.

Sample sequences were identified using sanger sequencing (Supplemental Information, "Validation Primers"). Bacterial samples with the correct resultant sequence were expanded via maxiprep and frozen in a glycerol stock. Extracted DNA could then be used in experiments, first with transient transfection into human embryonic kidney (HEK 293A) cells using lipofectamine to evaluate efficacy. HEK 293A cells do not contain a high level of endogenous 5-HT2 receptors and are not readily permissive to JCPyV infection. However, they are easily transfectable and were ideal for troubleshooting and initial evaluation of modified 5-HT2Rs.

After some troubleshooting, transient transfection of HEK 293A cells was achieved with all modified plasmids (Figure 9). Cells were grown in 24-well glass plates, after coating of the plate surface with Poly-L-Lysine to assist with cell adhesion, and transfected with lipofectamine. Because the plasmid is only expressed with the presence of doxycycline, 2 μg/mL doxycycline

was added to the cells after removal of lipofectamine. Cells were allowed to develop expression of the protein for 48 hours before imaging. Figure 9A shows a 5-HT2R+EBFP modified HEK 293A cell. This fluorescent microscopy image is of a live cell, because the 5-HT2A+EBFP was the last line to be established (due to troubleshooting limitations). Figure 9B shows a confocal microscopy maximum intensity projection image of a 5-HT2BR+mCherry modified HEK 293A cell which was fixed with 4% PFA and stained with DAPI. Confocal microscopy limits detected light to just one focal plane, which allows greater spatial resolution of the sample. When several planes are imaged, a complete three-dimensional image can be generated. With the confocal image, the cell membrane can be distinguished quite readily and sub-cellular details can be identified. Figure 9C shows another confocal microscopy maximum intensity projection image, this time of a 5-HT2CR+EGFP modified plasmid.

Figure 9A has little resolution, but expression of the modified 5-HT2R seems to be dispersed over the membrane. A similar effect can be seen in Figure 9C, where aside from several clumps of intense fluorescence (likely 5-HT2CRs which have been compartmentalized in cellular vesicles) there is fairly even expression of the receptors over the cell membrane surface, as would be expected. On the other hand, Figure 9B expression of 5-HT2BRs seems to be completely compartmentalized, with punctate fluorescent clumps in areas suggestive of sequestration of the receptor into endocytic compartments. This could be due to an effect of the mCherry protein link;

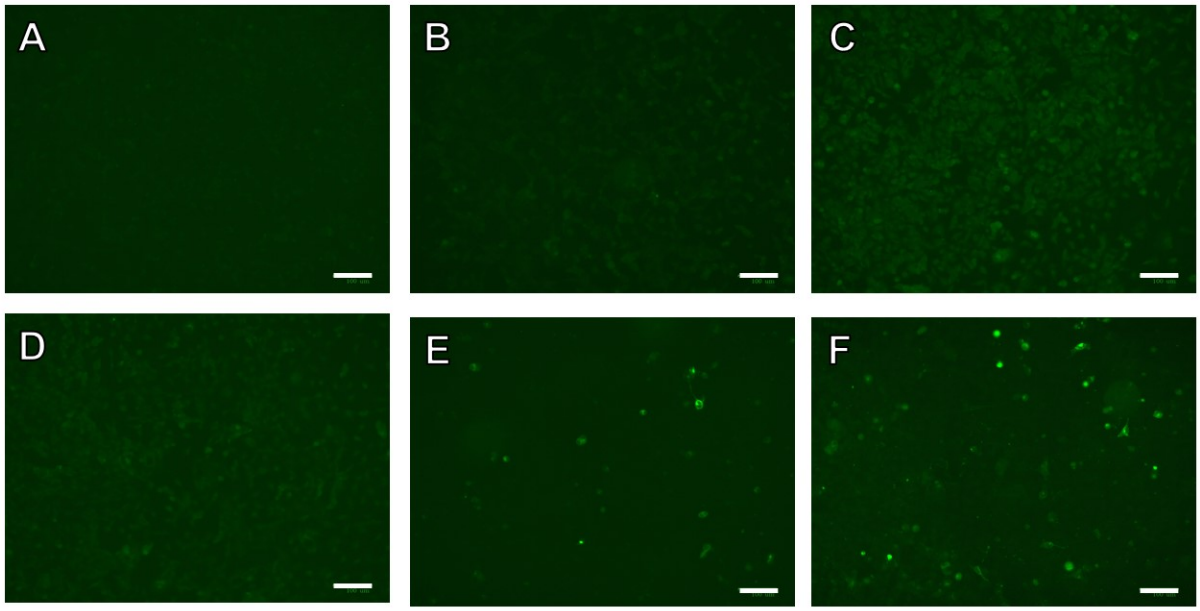

Figure 10. Time Course of Doxycycline-Induced 5-HT2CR+EGFP Expression
HEK 293A cells were evaluated for expression over a 48-hour period. Cells were grown on coverslips to confluency. Cells were placed in the presence of doxycycline for specified time periods before fixation of the cells and mounting on a microscope slide. Expression was evaluated with no doxycycline (A), doxycycline for 0 min (not shown), 15 min (not shown), 30 min (not shown), 1 hour (B), 2 hours (C), 3 hours (D), 24 hours (E), and 48 hours (F). Cells were imaged on a fluorescence microscope, and scale bars represent 100 µm.

although the fluorescent proteins are all about the same length and carry the same general protein structure, slight differences in nucleotide sequence between them may have rendered the 5-HT2B+mCherry receptor unable to traffic to the membrane.

Evaluation of Modified 5-HT2R Expression Characteristics

In order to ensure 5-HT2R expression was given enough time under doxycycline for appropriate receptor protein folding and trafficking to the cell membrane, expression was evaluated over a time course (Figure 10). The 5-HT2CR+EGFP plasmid was selected for transfection and expression because this was the only plasmid effectively working at the time, and it also had the most visible and consistent expression. HEK 293A cells were grown on Poly-

L-Lysine coated glass coverslips in a 24-well plastic plate. Once the cells reached 70% confluency, cells were transfected with 5-HT2C+EGFP and incubated for 4 hours with lipofectamine reagent. Media was replaced and cells were incubated an additional 8 hours for recovery. Doxycycline was then added to coverslips for set amounts of time before fixation and mounting on microscope slides. Time points included no doxycycline (as a control), doxycycline for 0 minutes (immediate fixation), 15 minutes, 30 minutes, 1 hour, 2 hours, 3 hours, 24 hours, and 48 hours. Previous work suggested expression could be seen in some proteins in as little as 30 minutes (Tet-On® Advanced Inducible Gene Expression Systems User Manual, see references). However, as this has to the lab's knowledge not been done in 5-HT2 receptors before, and some proteins may be produced much faster than others, time expression was expected to be different from predicted values.

No expression was seen before the 3 hour time point (Figure 10A, 10B and 10C show the no-doxycycline, 1 hour doxycycline and 2 hours doxycycline, respectively). After 3 hours, very low expression of the plasmid could be seen, but cell-specific expression was not clearly identified until 24 hours after induction. It is possible that some earlier expression could have been due to the presence of FBS in the cell media, as FBS appears to contain trace amounts of tetracycline derivatives capable of activating cell expression. However, this basal expression was not significant enough to warrant use of FBS-free media, as when this was done HEK 293A cells began to experience cellular stress and did not grow in a healthy phenotype (data not shown).

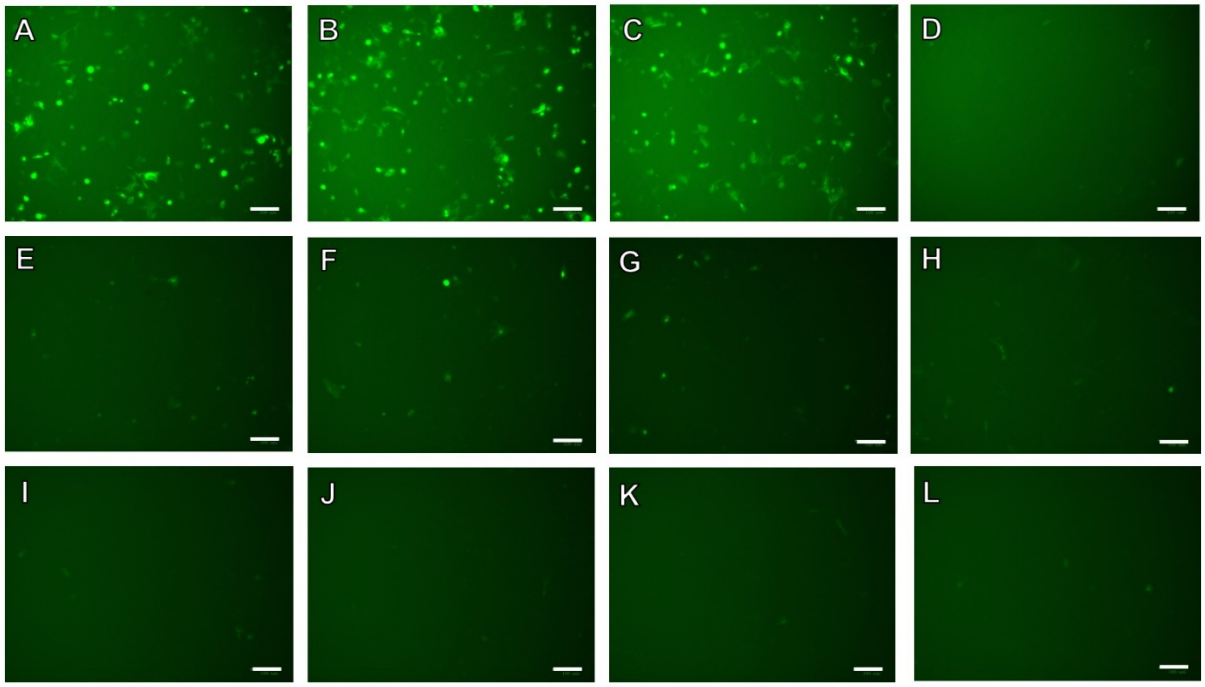

Figure 11. Dose Dependency of Doxycycline at 24 Hours
HEK 293A, SVGA and SVG2ABCKO cells were evaluated for expression of 5-HT2CR+EGFP after 24 hours in the presence of varying concentrations of doxyxycline. Cells were grown in a plastic 24-well plate to 70% confluency. Cells were placed in the presence of varying doses of doxycycline before fixation and imaging on a fluorescence microscope. Expression in HEK293A cells was evaluated with 0.5 µg doxycycline (A), 1 µg doxycycline (B), 2 µg doxycycline (C), or no doxycycline (D). 3 µg doxycycline was also evaluated (not shown). SVGA cells were evaluated at the same concentrations of doxycycline: 0.5 µg (E), 1 µg (F), 2 µg (G) or 0 µg (H). SVG2ABCKO cells were also evaluated for initial plasmid expression at the same concentrations: 0.5 µg (I), 1 µg (J), 2 µg (K) or 0 µg (L). Experiment was done prior to site-specific mutagenesis of plasmid. Scale bars represent 100 µm.

Figure 10F shows expression of 5-HT2CR+EGFP in HEK 293A cells after 48 hours of doxycycline exposure, and the clarity of expression, while only slightly more intense than in 10E (24 hours of doxycycline), assisted in designating 24 hours as the minimal time and 48 hours as the standard time for doxycycline expression post-transfection.

Because expression was not very different between 24 and 48 hours, cells were also evaluated for expression of 5-HT2CR+EGFP with varying concentrations of doxycycline. As above, HEK 293A cells were transfected with 5-HT2CR+EGFP and incubated with lipofectamine for 4 hours and without lipofectamine for 8 hours before addition of doxycycline. Doxycycline was

added at 0.5 µg/mL, 1 µg/mL, 2 µg/mL or 3 µg/mL and incubated an additional 24 hours, as this was established as a sufficient time period for expression. A negative control (no doxycycline) is also shown. This was repeated for SVGA cells and SVG2ABCKO cells. Figure 11 shows the dose dependency of doxycycline for HEK 293A cells (11A-11D), SVGA cells (11E-11H), and SVG2ABCKO cells (11I-11L). Negative controls are shown in the right-hand column. 1 µg/mL has more expression than 0.5 µg/mL, but about the same expression as 2 µg/mL, and 3 µg/mL is not shown as expression was similar to 2 µg/mL (Figure 11A-11C). HEK 293A cells have noticeably more expression of the 5-HT2CR+EGFP plasmid, which is to be expected because they are more readily transfectable than the other two cell lines. As was stated previously, some expression of the plasmid can be seen even with no addition of doxycycline, due to trace levels of tetracycline derivative present in FBS (Figure 11H).

Notably, SVG2ABCKO cells demonstrated no expression beyond basal fluorescence, even at 3 µg/mL doxycycline, which was indicative of a problem with plasmid expression. After examination of the cell line (which was a gift from Dr. Benedetta Assetta), a possible hypothesis was developed. Because the SVG2ABCKO cells were generated with CRISPR-Cas9 technology, they contained a guide RNA (gRNA) specific to a target sequence on the three serotonin receptors which triggered a double-stranded break and rendered the receptors nonfunctional. Because of this, the specific sequence had to be modified to reduce gRNA binding.

To accomplish site-directed mutagenesis of all three modified 5-HT2R plasmids, the Q5® Site-Directed Mutagenesis kit was used for a substitution reaction using non-overlapping primers as per protocol. The NEBaseChanger™ online tool was used to design primers (see Supplemental Information, “Site-Directed Mutagenesis Primers”). Primers were used in PCR to amplify the existing modified plasmid with the substitution of amino acids along the gRNA target site to produce the same protein sequence with differing codons (a completely silent mutation). These modified plasmids were then Sanger sequenced to ensure proper mutagenesis and used in production of stably transduced SVG2ABCKO cells, discussed below.

Genomic Integration of Modified 5-HT2Rs

Concurrently, stable transductions of HEK 293A and SVGA cells were attempted. Because SVGA cells are currently the best model for glial cell infection by JCPyV, they are ideal for receptor-virus interaction. However, these cells still contain endogenous 5-HT2Rs, which means the effect of transducing modified protein-linked receptors would likely be lost to the presence of non-tagged (less cumbersome) receptors. For this reason, SVG2ABCKO cells were selected as the target cell line for experimentation. While these lines were being produced, experimentation went onward with HEK 293A cells and SVGA cells to determine what preliminary data could be collected from these lines.

Stably transduced cells were generated through initial lentivirus production (outlined in

Methods) and infection with lentivirus containing the modified 5-HT2R plasmid (either 5-HT2AR+BFP, 5-HT2BR+mCherry, or 5-HT2CR+EGFP), a plasmid containing envelope proteins necessary for viral production, and a plasmid containing packaging proteins necessary for proper packaging of the virus. These genes were contained on three separate plasmids for safety, as lentiviruses without the proper safety checkpoints can be highly infectious to humans or other species. After infection with lentivirus, cells were selected in puromycin, a eukaryotic selection drug which should kill the cells which lack the resistance gene in the plasmid. After approximately 1 week of selection, cells were sorted on the Flow Activated Cell Sorter, a flow cytometer which can gate-select specific populations of fluorescing cells (Figure S1-S8). Cells were grown with antibiotic-antimycotic drugs, to prevent infection after exposure to open air for sorting. After this, cells were plated on a glass 24-well plate, induced with doxycycline for 24-48 hours, fixed with 4% PFA and imaged on the confocal microscope (Figure 12).

Figure 12 demonstrates the expression profiles of stably transduced and sorted HEK 293A cells with 5-HT2ABFP (Figure 12A), 5-HT2BR+mCherry (Figure 12B) and 5-HT2CR+EGFP (Figure 12C), as well as the same modified plasmids in SVGA cells. Interestingly, the morphology of receptor expression discussed previously is more apparent here; the 5-HT2BR+mCherry

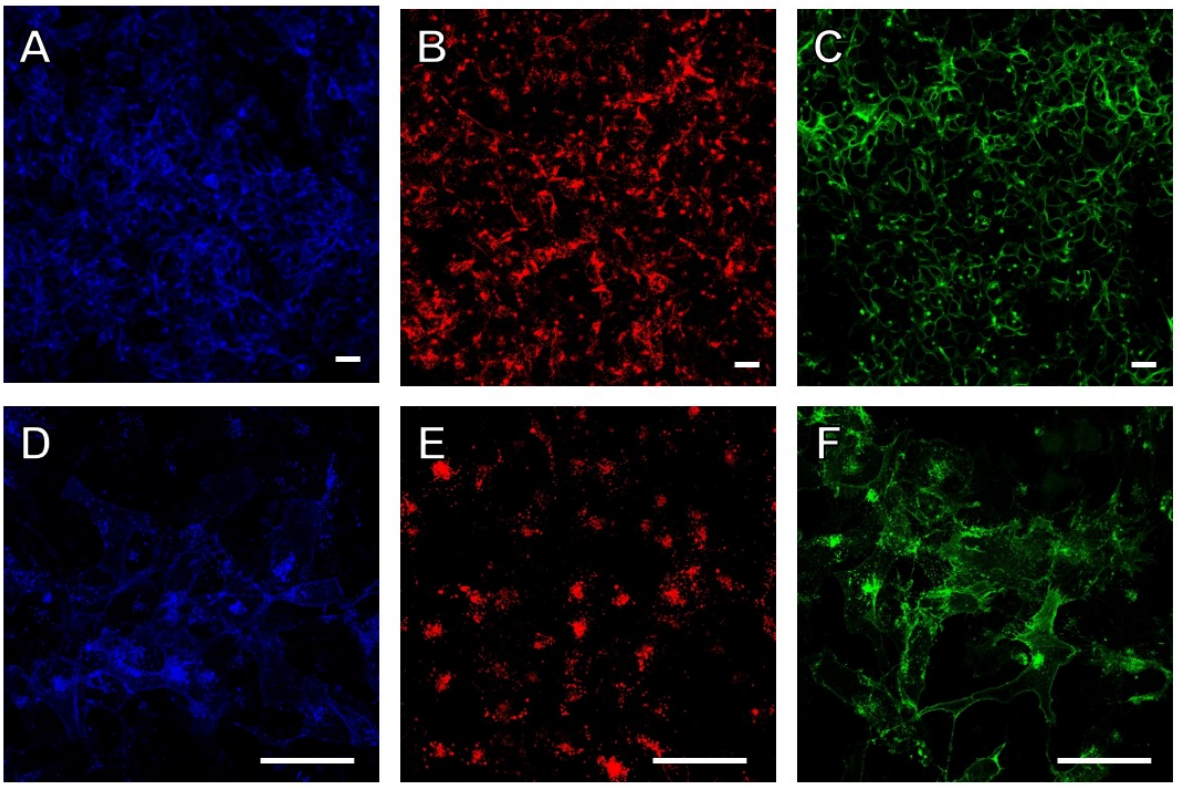

Figure 12. Stable Transduction of Single 5-HT2R Modified Plasmids
Lentiviruses were generated containing modified plasmids and used to infect and integrate the plasmid DNA stably into cell line genomes. Cells were selected with puromycin and sorted using Brown University's FACS machine. Cells were plated on a glass 24-well plate and fixed after 48 hours of doxycycline induction before confocal microscopy imaging. HEK 293A cells were transduced with 5-HT2AR+EBFP (A), 5-HT2BR+mCherry (B) or 5-HT2CR+EGFP (C). SVGA cells were transduced with 5-HT2AR+EBFP (D), 5-HT2BR+mCherry (E), or 5-HT2CR+EGFP (F). Scale bars represent 50 μm.

receptor in both HEK 293A and SVGA cells has little membrane expression relative to the 5-HT2AR+EBFP or 5-HT2CR+EGFP receptors (Figure 12).

Because the stably transduced HEK 293A and SVGA cells express 5-HT2Rs which are tagged with fluorescent proteins, there is no requirement for immunochemistry or fixation in order to visualize the receptor location. This allows the option to do experimentation on live cells, given appropriate microscopy techniques can be used. Live cells were imaged after successful 5-

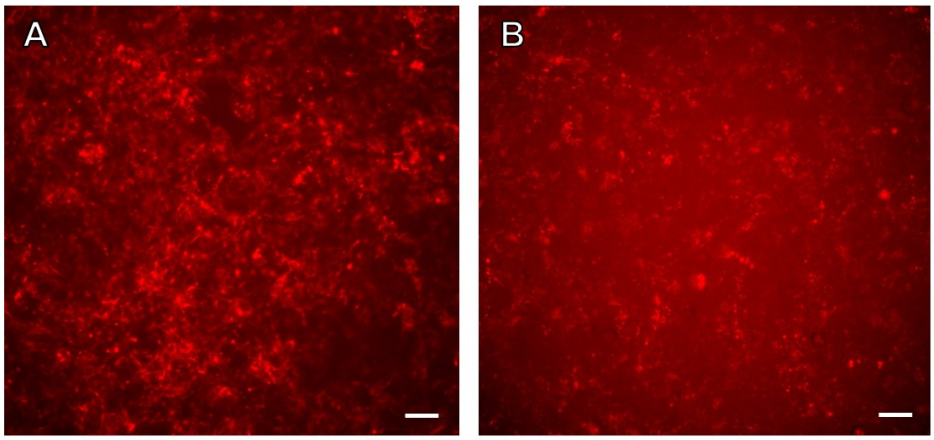

Figure 13. Stable Transduction of Single 5-HT2R Modified Plasmids
Lentiviruses were generated containing modified plasmids and used to infect and integrate the plasmid DNA stably into cell line genomes. Cells were selected with puromycin and sorted using Brown University's FACS machine. Cells were plated in a 24-well glass plate and induced with doxycycline for 48 hours before fluorescence microscopy. Due to the low quality of images in Figure 12, 5-HT2BR+mCherry images were taken in live HEK 293A (A) and SVGA (B) cells. Scale bars represent 100 µm.

HT2BR+mCherry transduction because confocal microscopy was not able to capture the magnitude of cellular expression adequately (Figure 13). Potential experiments which are now possible include tracking the location of 5-HT2Rs during infection in the same cell population at specific time points, to visualize exactly how the receptors interact with JCPyV on a more fluid level.

Double Expression of Modified 5-HT2Rs

Once single transductions were deemed successful, these cells were used to generate double-transfected lines. Cells with 5-HT2CR+EGFP were additionally infected with 5-HT2AR+EBFP or 5-HT2BR+mCherry, due to the consistency and reliability of 5-HT2CR+EGFP expression. Cells transduced with 5-HT2AR+EBFP were additionally transduced with 5-HT2BR+mCherry, because the 5-HT2AR+EBFP seemed to have consistently membranous expression, and so served as an adequate base for a second transduction. These combinations are shown in Figure 14 for HEK 293A cells, which were the first cell type attempted. Figure 14A

and 14B show 5-HT2AR+EBFP and 5-HT2CR+EGFP, respectively, in the same cell line (HEK 2A-2C) after sorting and induction with doxycycline on a fluorescent microscope. The fluorescence microscope did not display the blue channel (EBFP) expression well, but confocal microscopy of receptor expression can be seen in later figures. Figure 14C and 14D show 5-HT2BR+mCherry expression with 5-HT2CR+EGFP expression in the same cell line (HEK 2B-2C). Lastly, Figure 14E and 14F show expression of 5-HT2AR+EBFP and 5-HT2BR+mCherry, respectively, in the same cell line (HEK 2A-2B). This combination of

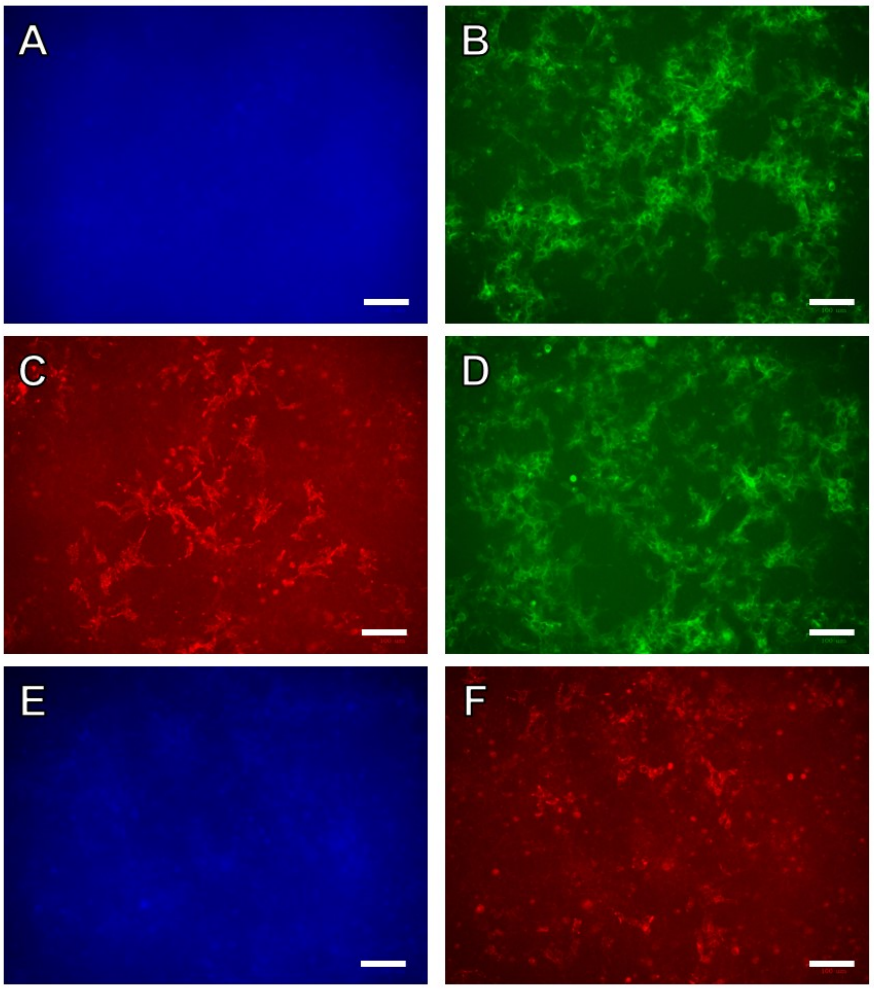

Figure 14. Stable Transduction of Double 5-HT2R Modified Plasmids in HEK 293A Cells
Lentiviruses were generated containing modified plasmids and used to infect and integrate the plasmid DNA stably into cell line genomes. HEK 293A cells were selected with puromycin and sorted using Brown University's FACS machine. Live cells were imaged using fluorescence microscopy after 48 hours of doxycycline induction. Color channels were imaged separately for clarity. HEK-2A2C cells were transduced with 5-HT2AR+EBFP (A) and 5-HT2CR+EGFP (B), HEK-2B-2C cells were transduced with 5-HT2BR+mCherry (C) and 5-HT2CR+EGFP (D). HEK-2A2B cells were transduced with 5-HT2AR+EBFP (E) and 5-HT2BR+mCherry (F). Scale bars represent 100 μm.

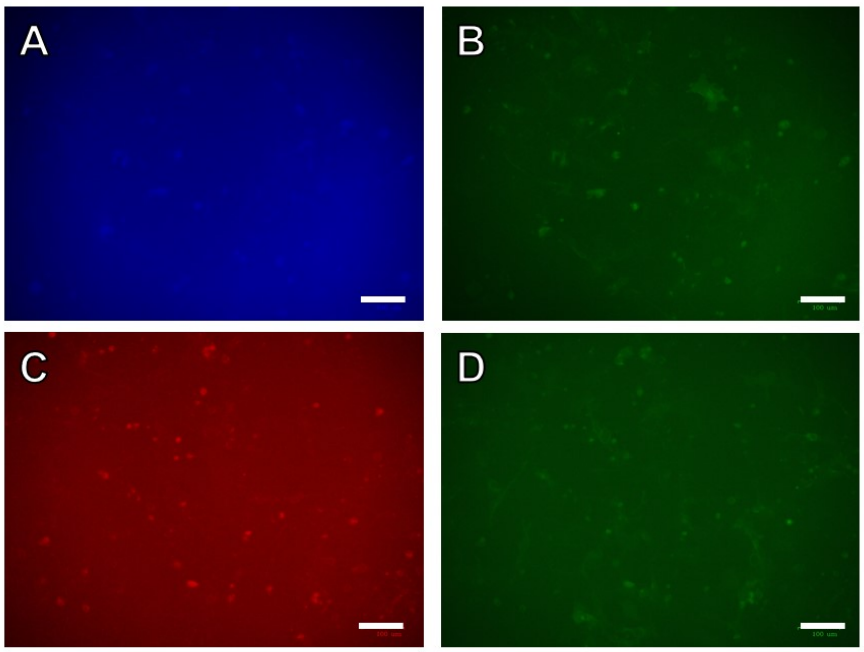

Figure 15. Stable Transduction of Double 5-HT2R Modified Plasmids in SVG2ABCKO Cells
Lentiviruses were generated containing modified plasmids and used to infect and integrate the plasmid DNA stably into cell line genomes. SVG2ABCKO cells were selected with puromycin and sorted using Brown University's FACS machine. Live cells were imaged using fluorescence microscopy after 48 hours of doxycycline induction. Color channels were imaged separately for clarity. SVGKO-2A2C cells were transduced with 5-HT2AR+EBFP (A) and 5-HT2CR+EGFP (B) and SVGKO-2B-2C cells were transduced with 5-HT2BR+mCherry (C) and 5-HT2CR+EGFP (D). SVGKO-2A2B cells were lost to infection prior to imaging. Scale bars represent 100 µm.

double transductions (2A-2C, 2B-2C and 2A-2B) ensured combination of all receptors with the highest probability of successful expression patterns based on previous cell line analysis.

After site-directed mutagenesis of the 5-HT2R plasmids, stable transduction was attempted in SVG2ABCKO cells. Unfortunately, these cells were affected heavily by yeast and bacterial infections and little data could be collected from them before they were lost. After single transductions and sorting (as described previously), SVG2ABCKO cells were double transduced as the HEK 293A cells had been. Figure 15 shows some images of the resulting cells which were expressing successfully at low levels. Although the fluorescence microscopy images are not especially descriptive, FACS sorting data shows a cell population of 5-HT2BR+mCherry and 5-

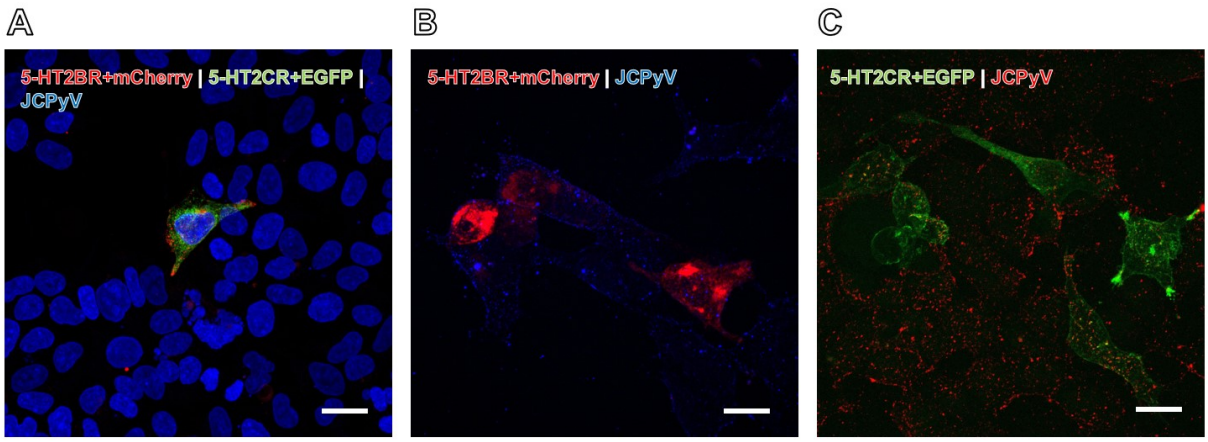

Figure 16. Double Transfection and Labeled JCPyV
HEK 293A cells were transiently transfected with either 5-HT2BR+mCherry (B), 5-HT2CR+EGFP (C) or both (A) and induced with doxycycline for 48 hours. (A) shows a successfully double-transfected cell post-fixation and DAPI staining. HEK 293A cells were serum starved for 24 hours in the presence of doxycycline before undergoing JCPyV binding experiment. 405-labeled JCPyV was used to infect cells transfected with 5-HT2BR+mCherry (B) for 5 minutes before fixation. 633-labeled JCPyV was used to infect cells transfected with 5-HT2CR+EGFP (C) for 5 minutes before fixation. Scale bars represent 20 µm.

HT2CR+EGFP expressing cells were successfully identified (Figure S8).

Because of the time-consuming nature of stable cell line generation, transient transfections were used in the meantime to examine potential techniques for JCPyV research. Double transfections of both 5-HT2BR+mCherry and 5-HT2CR+EGFP plasmids were used in conjunction with fluorescent protein-tagged JCPyV (produced prior to experiment by the Atwood lab). HEK 293A cells were transfected on a glass 24-well plate and induced with doxycycline for 48 hours and were without FBS for 12 hours (a serum starved state which promoted trafficking of receptors to the cell surface) before infection with tagged JCPyV. Prior to infection, cells were chilled on ice to solidify cell membranes and prevent entry of the virus into the cell. On ice, tagged JCPyV was added to the cells and incubated for 1 hour to allow for viral binding to cellular receptors. The cells were then warmed to 37C for 5 minutes before fixation. This allowed the virus

to begin cellular entry, but prevented the virus from reaching later stages of infection.

Based on Assetta et al. (2013 and 2019), JCPyV interacts with 5-HT2Rs between 5 and 15 minutes post infection, so this method of pre-chilling the cells allowed capture and fixation of infection at the 5 minute time point across the entire cell membrane. Cells with expression of both 5-HT2BR+mCherry and 5-HT2CR+EGFP plasmids can be seen with DAPI staining in Figure 16A. To determine which JCPyV tag would be more conducive to this experiment, cells were tested with both a 405 nm-emission wavelength tagged JCPyV (Figure 16B) and 633 nm-emission wavelength tagged JCPyV (Figure 16C). For Figure 16B and 16C, only single transfections of 5-HT2BR+mCherry (Figure 16B) or 5-HT2CR+EGFP (Figure 16C) were used to allow identification of tagged JCPyV more easily. 405 nm emission wavelength-tagged JCPyV, or 405-JCPyV, seemed to have more easily identifiable expression and was more stable relative to 633 nm emission wavelength-tagged JCPyV, or 633-JCPyV (Figure 16B and 16C). The 633-JCPyV had more disperse expression, which could have represented background levels of expression. On the other hand, 405-JCPyV clustered around cellular membranes (and not cytosol) as would be expected for virus bound to cellular membranes, considering the infection was fixed at 5 minutes.

Modified 5-HT2R Effect on JCPyV Infection

Although the fluorescent protein tags for modified plasmids were attached at the C-terminus of the 5-HT2R sequence and so would be intracellular, it is possible that addition of the

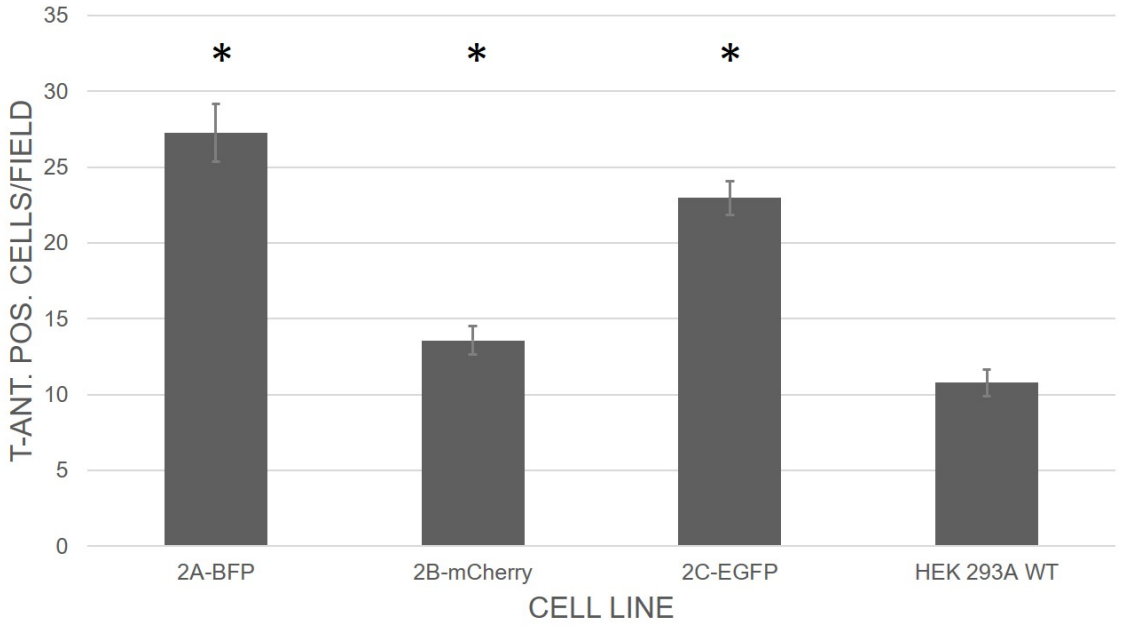

Figure 17. JCPyV Infection of Modified HEK 293 Cells
HEK 293A cells were stably transduced with 5-HT2AR+EBFP (2A-BFP), 5-HT2BR+mCherry (2B-mCherry), or 5-HT2CR+EGFP (2C-EGFP). After doxycycline induction for 48 hours, cells were infected with JCPyV over a five-day period. After five days, cells were fixed and stained for the presence of T-Antigen. T-Antigen positive cells were counted using fluorescence microscopy and compared to control HEK 293A (HEK 293A WT). All modified cell lines had an increase in T-Antigen positive cells versus control (two-tailed T-Test, $p < 0.05$). Error bars show Standard Error.

tag could affect the ability of JCPyV to infect the modified cells. To determine the effect of the tag on JCPyV infection, HEK 293A cells were transfected with each of the three modified plasmids (Figure 17). Because HEK 293A cells do not typically express high levels of 5-HT2Rs, and JCPyV is partially dependent on 5-HT2Rs for infection, it would be expected that addition of the modified plasmids would increase the ability of JCPyV to infect the HEK cells, represented by an increase in the population of infected cells. In HEK 293A cells, VP1 is not produced, so instead the early gene T-antigen is used as a marker for infected cells.

HEK 293A stably-transduced cells were grown on glass 24-well plates which were coated

with Poly-L-Lysine for 1 hour prior to addition of cells. 5-HT2AR+EBFP-modified HEK cells, 5-HT2BR+mCherry-modified HEK cells and 5-HT2CR+EGFP-modified HEK cells were induced with doxycycline for 24 hours before infection with JCPyV and incubation with JCPyV over a 5 day period. Although the infection cycle of JCPyV is typically only about 3 days in SVGA cells, HEK 293A cells are poorly permissive and so an extended period of incubation was deemed necessary. Once this period was over, cells were fixed in 100% ice-cold ethanol, which was previously identified as the best method for T-antigen staining by Dr. Bethany O'Hara. Cells were immunostained for T-antigen using laboratory anti-T-antigen antibody and stained with DAPI to ensure visualization fields were composed of approximately equivalent numbers of cells. Cells were imaged using a Nikon Ti2 fluorescence microscope which used an automatic cell counting software developed by Nikon. This software was not used here to count T-antigen, as T-antigen staining could not easily be counted by computer. The software was, however, utilized to ensure a consistent approximate number of cells per field based on DAPI cell counts. The number of T-antigen positive cells per field were quantified for each condition, and a two-tailed T-test performed relative to control condition (wild-type HEK 293A) to determine significance (Figure 17). All three modified cell lines exhibited a significant increase in infection relative to the control. 5-HT2AR+EBFP modified HEK cells had a p value of 1.85×10^{-10}, 5-HT2BR+mCherry modified HEK cells had a p value of 0.036, and 5-HT2CR+EGFP modified HEK cells had a p value of 7.79

x 10^{-12}. The 5-HT2BR modified cells were least significant, possibly because of receptor sequestration in endocytic compartments preventing the cells from being infected by JCPyV. However, it is important to note that there was still a slight increase in infection in this line, suggesting that perhaps the 5-HT2BR+mCherry does traffic to the membrane in low numbers. Overall, this data suggests that without the presence of endogenous receptors, the modified 5-HT2R stably integrated (transduced) plasmids do mediate JCPyV infection.

Stably transduced SVGA cells were also produced, and evaluated for JCPyV infection efficiency. In order to investigate the efficacy of a control transduction containing only GFP, another line infected with the pLKO.1 GFP control lentivirus was selected. Because SVGA cells have endogenous 5-HT2Rs, one could hypothesize an additive effect of integrating modified 5-HT2Rs into the genome. At the same time, depending on how the gene is integrated and how the resulting tagged receptors affect normal 5-HT2R processing, it is possible that a reduction in JCPyV infection could also be seen. SVGA cells are fully permissive to JCPyV and so will produce VP1 during viral replication. Because of this, anti-VP1 antibodies were used to identify infected cells. As with the HEK 293A cells, modified SVGA cells were plated, induced and infected, but this time fixed in 100% ice-cold methanol. Cells were incubated with virus for 3 days instead of 5 to prevent viral lysis of cells. After fixation, cells were immunostained for VP1 and with DAPI (to identify numbers of cells per field). Plates were imaged on a Nikon Ti2 fluorescence microscope

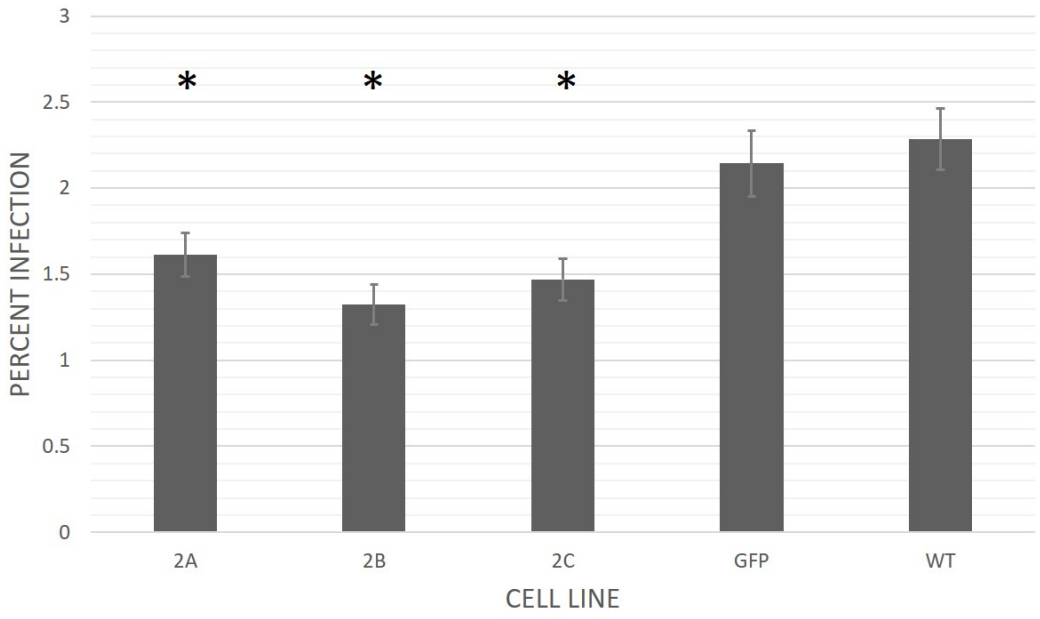

Figure 18. JCPyV Infection of Modified SVGA Cells
SVGA cells were stably transduced with 5-HT2AR+EBFP (2A), 5-HT2BR+mCherry (2B), or 5-HT2CR+EGFP (2C). After doxycycline induction for 48 hours, cells were infected with JCPyV. After three days, cells were fixed and stained for the presence of VP1. VP1-positive cells were counted using fluorescence microscopy and Nikon cell counting software. Percentages were calculated based on DAPI staining. There was a decrease in percent infection of modified SVGA cells relative to both controls, pLKO.1 GFP (GFP) and SVGA (WT), (two-tailed T-Test, $p < 0.05$). Error bars represent Standard Error.

and counted using a program written by Nikon. Percent of infection was determined from these data and two-tailed T-tests run on each condition relative to wild-type SVGA cells.

Interestingly, there was a significant decrease in JCPyV infection in SVGA cells modified with tagged 5-HT2Rs, but not the pLKO.1 GFP modified cells (Figure 18). The p-values for each modified 5-HT2R cell line were far below 0.05, as follows: 5-HT2AR+EBFP $p = 0.0032$, 5-HT2BR+mCherry $p = 2.55 \times 10^{-5}$, and 5-HT2CR+EGFP $p = 0.00034$. Because the control plasmid was not significantly different from the wild type SVGA cells ($p = 0.59$, two-tailed T-test), the process of lentiviral transduction did not seem to affect the permissivity of the cells to JCPyV.

However, it is unknown why the addition of modified 5HT2Rs led to a decrease in JCPyV infection. One possible explanation could be that expression of the modified protein could inhibit (directly or indirectly) expression of the endogenous receptors, leading to fewer 5-HT2Rs overall for the virus to interact with, possibly through competition between the endogenous and modified receptors. Another potential explanation could be that the modified 5-HT2Rs were inserted at a location in the genome which led to downregulation of 5-HT2R expression. Repeating this experiment in stably transduced SVG2ABCKO cells would determine whether the effect is due to issues with the modified 5-HT2Rs or to the presence of endogenous 5HT2Rs.

Visualization of 5-HT2R Response to Ligand Binding

In order to determine in part whether the modified 5-HT2Rs respond as expected to the binding of JCPyV as well as other ligands, HEK 293A cells were double-transfected with 5-HT2BR+mCherry and 5-HT2CR+EGFP. These cells underwent the ligand binding experiment detailed in the methods, where cells were pre-chilled and incubated with the ligand before heating to 37C and fixation at a specific time point. Cells were incubated with plain media (control), 405-JCPyV or serotonin (5-HT) for 0 minutes, 5 minutes, 10 minutes and 15 minutes before fixation with 4% PFA (data at 5 minutes shown in Figure 19). Addition of plain media did not change the morphology of 5-HT2R expression; 5-HT2BR+mCherry had a punctate, vesicularized morphology while 5-HT2CR+EGFP had even expression over the cell surface (Figure 19A and 19D).

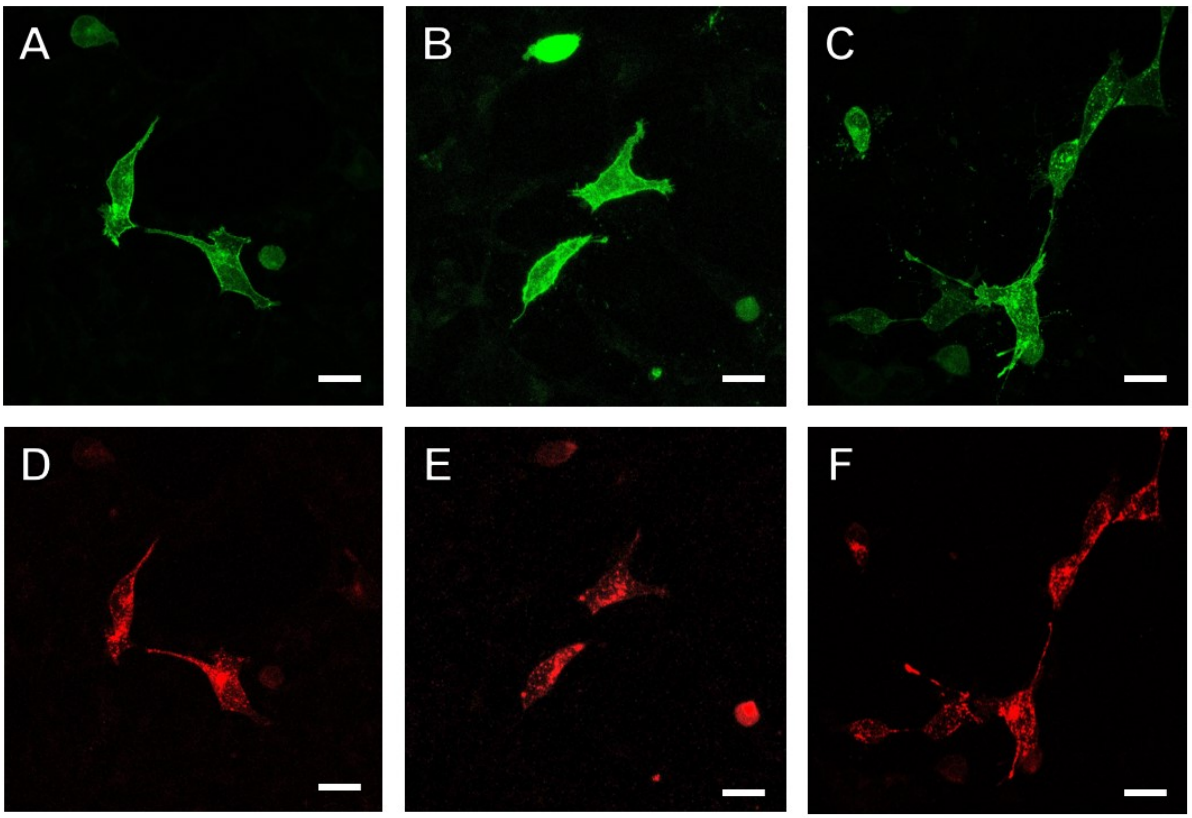

Figure 19. Ligand Binding Affects 5-HT2R Expression
HEK 293A cells were double-transfected with 5-HT2BR+mCherry and 5-HT2CR+EGFP. Cells were plated with doxycycline at 1 µg/mL. Cells were pre-chilled for ligand binding, and media replaced with either plain (control) media (A and C), 403-labeled JCPyV at 1:30 dilution from lysate (B and E) or 5-HT ligand at 10 µM (C and F). (A-C) show expression of 5-HT2CR+EGFP, while (D-F) show expression of 5-HT2BR+mCherry. Cells were incubated on ice with ligand for 1 hour, then placed at 37C for ligand entry for 5 minutes before fixation. Data for 0 minutes, 15 minutes, 30 minutes and 1 hour not shown. Scale bars represent 20 µm.

Addition of either 405-JCPyV or 5-HT did not seem to significantly change 5-HT2BR+mCherry expression morphology, which was expected because the sequestered receptors may no longer be affected by surface ligands (Figure 19E and 19F). Addition of 405-JCPyV seemed to lead to dense receptor expression at the cell surface at a level higher than that of basal expression, possibly due to interaction between receptors and JCPyV. However, because only a single image is shown, more data is needed for a complete conclusion (Figure 19B).

Addition of 5-HT to 5-HT2CR+EGFP led to apparent endocytosis of receptors (with receptor clumping similar to that seen in 5-HT2BR+mCherry expression), which was expected as 5-HT2Rs will be internalized upon binding to serotonin (Figure 19C, Raote et al. 2007). This indicates that the 5-HT2CR+EGFP modified receptors do not seem to be inhibited in early stages of cellular response by the protein tag.

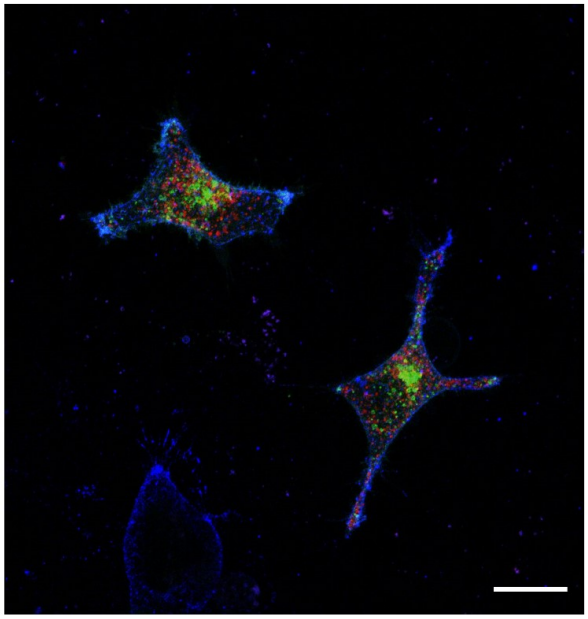

Figure 20. Colocalization of 5-HT2R with Labeled JCPyV
HEK 293 cells were double-transfected with 5-HT2BR+mCherry and 5-HT2CR+EGFP. Cells were pre-chilled on ice for viral binding and JCPyV added for 1 hour at 1:30 dilution from lysate. Cells were moved to 37C for either 0 minutes (immediate fixation), 5 min, 15 min (shown above), 30 min or 1 hour. Scale bar represents 20 µm.

Specific Interactions Between 5-HT2R Variants and JCPyV

Lastly, the same cells were examined for interactions between JCPyV and 5-HT2Rs. It is possible that receptors may heterodimerize or homodimerize with the virus, but the nature of this interaction is not known. Understanding the relationship between the three receptors during viral infection could lead to potential checkpoints at which to inhibit JCPyV infection. 405-JCPyV was imaged in conjunction to cells expressing both 5-HT2BR+mCherry and 5-HT2CR+EGFP as an initial stage of exploration into the subject (Figure 20). This maximum intensity projection suggests potential interactions between receptors and virus, but little interaction between endocytosed receptors in the cytosol.

However, because this was a single image, more analysis was needed.

In order to determine in a quantitative (and unbiased) way whether 5-HT2Rs heterodimerize to a greater extent during JCPyV infection, indicating higher levels of interaction potentially between only certain receptors in the presence of virus, a preliminary colocalization analysis was completed on HEK 293A cells which had been stably transduced with a combination of two modified 5-HT2Rs.

HEK 293A cells containing stably transduced combinations of 5-HT2AR+EBFP with 5-HT2BR+mCherry, 5-HT2AR+EBFP with 5-HT2CR+EGFP, or 5-HT2BR+mCherry with 5-HT2CR+EGFP were plated on Poly-L-Lysine coated coverslips in a 24 well glass plate. Cells were induced with doxycycline for 48 hours before ligand binding. JCPyV lysate, SV40 or Plain media were added to cells on ice and warmed to 37C for 5 minutes before fixation with 4% PFA. SV40 was used as a control because it does not interact with serotonin receptors (Assetta et al. 2019, Morris-Love et al. 2019). Plain media was used as a secondary control to evaluate whether SV40 may have a different effect relative to no ligand at all. Cells were fixed and coverslips mounted on microscope slides. Because of the nature of colocalization analysis, careful precautions were considered in imaging. The confocal microscope was set to specific gain and intensity levels for each channel, and then was maintained at those levels for all conditions. Images of each condition were collected for analysis.

Colocalization can be evaluated by evaluating proportionally the ratio of fluorescence in colocalizing pixels of two different color channels, known as Mander's split coefficient. This coefficient ranges from 0 to 1, with 1 indicating a perfect 1:1 ratio of fluorescence intensity between the channels (Manders et al. 1993). Colocalization can also be evaluated with Pearson's correlation coefficient, which evaluates correlational colocalization without being affected by signal intensity. Pearson's coefficient ranges from -1 to 1, where 0 indicates no correlation, +1 indicates perfect positive correlation, and -1 indicates perfect negative correlation between the fluorescence in the color channels (Dunn et al. 2011). Images from confocal microscopy were evaluated using Fiji ImageJ's plugin, Coloc2. A region of interest containing the double-expressing cell was outlined, and point spread function calculated for each channel using the Colocalization plugin. Images were thresholded using Costes regression, and 20 iterations of Costes randomizations were used to generate data for each image z-stack. Between 3 and 6 images were taken for each condition, and resulting Mander's and Pearson's coefficients examined in an excel spreadsheet. Mean Mander's coefficients (above the threshold of the channel 1 image) were graphed and significance tests run (Figure 21). Mander's coefficients were calculated by comparing to the channel containing information from the 5-HT2R which was transduced first and thus underwent complete sorting and selection (either 5-HT2AR+EBFP or 5-HT2CR+EGFP, depending on the cell line). This was because this channel was more likely to contain generalized

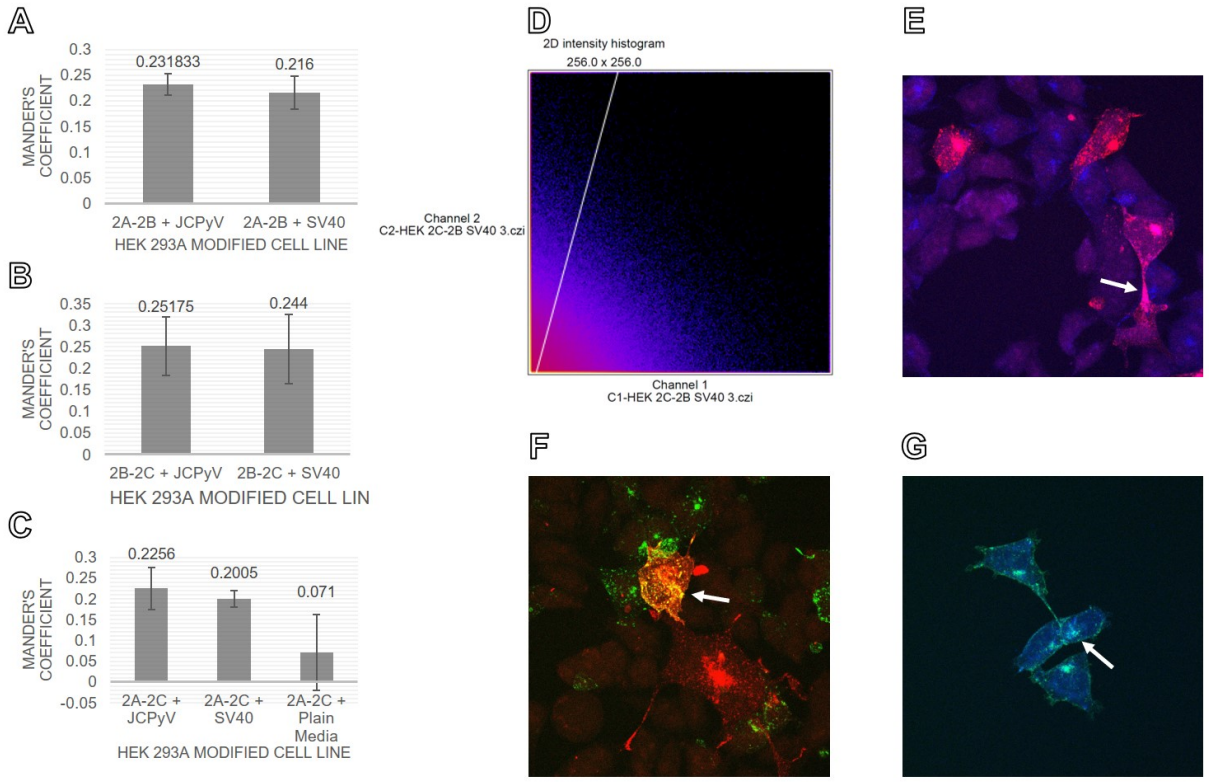

Figure 21. Colocalization of 5-HT2R with JCPyV in Double-Modified HEK 293A Cells
HEK 293A cells were stably modified with two labeled 5-HT2R receptors. After induction and binding to either JCPyV, SV40 (a control) or Plain Media (a control), cells were fixed at 5 min post ligand binding and imaged on a confocal microscope. Images of double-labeled cells were collected and evaluated for colocalization using Fiji ImageJ's Coloc2 plugin. Mander's split coefficients were calculated post-thresholding and are displayed above for cells expressing 5-HT2AR+EBFP and 5-HT2BR+mCherry (A), 5-HT2BR+mCherry and 5-HT2CR+EGFP (B) and 5-HT2AR+EBFP and 5-HT2CR+EGFP (C). A representative 2D intensity plot is shown in (D), indicating intensity overlap between the two color channels. Representative images for (A), (B) and (C) are shown in (E), (F) and (G), respectively. (E) displays 5-HT2AR+EBFP with 5-HT2BR+mCherry in the presence of SV40. (F) shows 5-HT2BR+mCherry with 5-HT2CR+EGFP in the presence of JCPyV. (G) shows 5-HT2AR+EBFP with 5-HT2CR+EGFP in the presence of plain media. White arrows in (E-G) indicate potential areas of colocalization. N ≥ 3 images per condition, and images were collected in z-stacks of 8-15 images. P > 0.05 for all data. Error bars represent Standard Error.

expression of the receptors across all cells.

There was no statistical significance between colocalization of receptors in any cell line (Figure 21A-21C). Figure 21A shows the Mander's coefficients for cells expressing both 5-HT2AR+EBFP and 5-HT2BR+mCherry in the presence of JCPyV (+JCPyV) or SV40 (+ SV40) (P = 0.066). Corresponding Pearson's coefficients were -0.2 in the presence of JCPyV and -0.19 in the presence of SV40 (P = 0.846). Figure 21B shows Mander's coefficients for cells expressing

both 5-HT2BR+mCherry and 5-HT2CR+EGFP in the presence of JCPyV or SV40 (P = 0.242). Corresponding Pearson's coefficients were 0.005 in the presence of JCPyV and 0.12 in the presence of SV40 (P = 0.527). Figure 21C shows Mander's coefficients for cells expressing 5-HT2AR+EBFP and 5-HT2CR+EGFP in the presence of JCPyV, SV40 or Plain Media. Statistical T-tests were done with comparison to SV40 data (P = 0.687 for JCPyV and P = 0.546 for Plain Media). Corresponding Pearson's coefficients were -0.174 in the presence of JCPyV (P = 0.046), -0.33 in the presence of SV40 (Control) and -0.16 in the presence of Plain Media (P = 0.068). It is likely that additional data would provide enough information to determine whether an actual effect can be seen in receptor colocalization. A representative 2D intensity histogram of cells from the analysis in Figure 21B after addition of SV40 shows little colocalization between channels (Figure 21D). Maximum intensity projection images can be seen in Figure 21E-21G, and white arrows indicate areas where potential colocalization might occur. These images are for visualization purposes only and do not serve for analysis, as the condensed stack is missing spatial information which is important for distinguishing true colocalization. However, the preliminary data shown in Figure 21 could potentially serve to predict how additional data might shape hypotheses.

There does not seem to be a significant difference in colocalization between any of the receptor pairs compared to SV40, but there was a consistent trend for slightly less colocalization

(a smaller Mander's coefficient) in all SV40 conditions (Figure 21A-C). It is possible that this effect could become significant with additional data, even though it is small. In addition, the only condition with plain media (Figure 21C) curiously had a much lower Mander's coefficient, although this was not significant. Further analysis of colocalization coefficients may be helpful, as the Pearson's coefficients may also be informative in determining the presence of heterodimerization between receptors. Lastly, it is possible that heterodimerization between receptors occurs with equal frequency with or without JCPyV, which would suggest that either JCPyV does not discriminate between 5-HT2Rs or it may be possible that homodimerizations between receptors are more important in JCPyV infection.

Discussion

By generating inducible, selectable and stable cell lines containing modified versions of the 5-HT2A, 5-HT2B and 5-HT2C receptors linked to fluorescent proteins, this study has (1) provided a method by which to precisely track the location of 5-HT2Rs, even in live cells, and (2) gathered data to support the hypothesis that tagging the GPCR 5-HT2 receptor with a C-terminal protein does not significantly affect receptor function. In addition, this study has begun preliminary exploration into how 5-HT2Rs interact with each other in the presence or absence of JCPyV, which could lead to significant findings relating to JC viral biology. It is likely that additional data will lead to clearer answers with regards to how 5-HT2Rs interact with JCPyV during infection. 5-HT2Rs likely act individually, and probably do heterodimerize in at least some configurations, but may also form homodimers (Assetta et al. 2019). This study is consistent with the hypothesis that JCPyV induces homodimerization of 5-HT2Rs, as heterodimerization has as of yet not been identified in the data as a direct result of JCPyV infection (Figure 19, Figure 21).

HEK 293A cells were used as a proxy for SVGA cells in order to accomplish more complete data collection; use of the SVG2ABCKO cell line (with no endogenous 5-HT2 receptors) likely would act as the most accurate model for this research. Future directions will include the completion of double-transduced SVG2ABCKO cell line generation. Although trimerization of the receptors is unlikely considering they can act independently to rescue JCPyV infection (Assetta

et al. 2019), a triple-modified SVG2ABCKO cell line containing all modified plasmids stably integrated into the cell genomes would likely be the most accurate model for evaluating JCPyV infection in the human brain.

Beyond generation of additional cell lines, the most pressing step forward is to complete colocalization analysis of cell lines. Additional data collection and analysis is necessary to determine the significance of the preliminary results shown in Figure 21. The main purpose of the study is to work toward understanding the interactions between 5-HT2Rs and JCPyV. Using these cell lines to determine receptor interactions would provide a clearer understanding of viral biology, and may influence development of drugs or treatments to slow or prevent JCPyV infection in the brain. In addition, these cell lines have a wide application outside of receptor interactions on the cell surface.

Another way to determine whether 5-HT2Rs interact through hetero- or homodimerizaiton is through immunoprecipitation of 5-HT2R proteins from cell lysate and subsequent western blot analysis of intracellular protein interactions. Although the 5-HT2Rs do not have specific antibodies available to be used in this process, the fluorescent tags to which they are attached do have specific antibodies available. Examining the immunostained western blot of cell lysate from, for example, triple-transduced SVG2ABCKO cells (containing all three modified 5-HT2Rs), may indicate whether two or more of the receptor subtypes co-

immunoprecipitate naturally or with the addition of JCPyV. Similarly, a pull-down assay (like immunoprecipitation, except using one of the modified 5-HT2Rs or a strong ligand instead of an antibody) would also indicate whether these interactions occur. Though these two methods would be immensely helpful in determining the status of 5-HT2R interaction, they are often difficult to accomplish and may not detect weak or very transient interactions between proteins. One more possible avenue to explore is Fluorescence Resonance Energy Transfer (FRET), in which the proximity of two unique fluorophores causes the excitation of one to induce excitation and emission in the other. Because the proximity required for this transfer of energy to occur is very small, the detection of the second fluorophore would likely indicate protein interaction.

Because the stable generation of these cell lines ensures expression of fluorescent proteins while cells are still living, the intracellular location of 5-HT2Rs can be tracked in real time, opening the possibility for time course studies involving receptor trafficking in a single population of cells, rather than fixing cells at varying time points. This has application both for understanding JCPyV infection and beyond, without risking the loss of information during fixation. JCPyV undergoes a shift between cytosolic pathways during infection, and the mechanism for this shift is unknown. One hypothesis is that 5-HT2Rs are involved in this shift, a question which can be resolved using the tagged 5-HT2Rs generated in this study. In addition, 5-HT2Rs have an extremely wide breadth of action across the brain and throughout the body, which means that

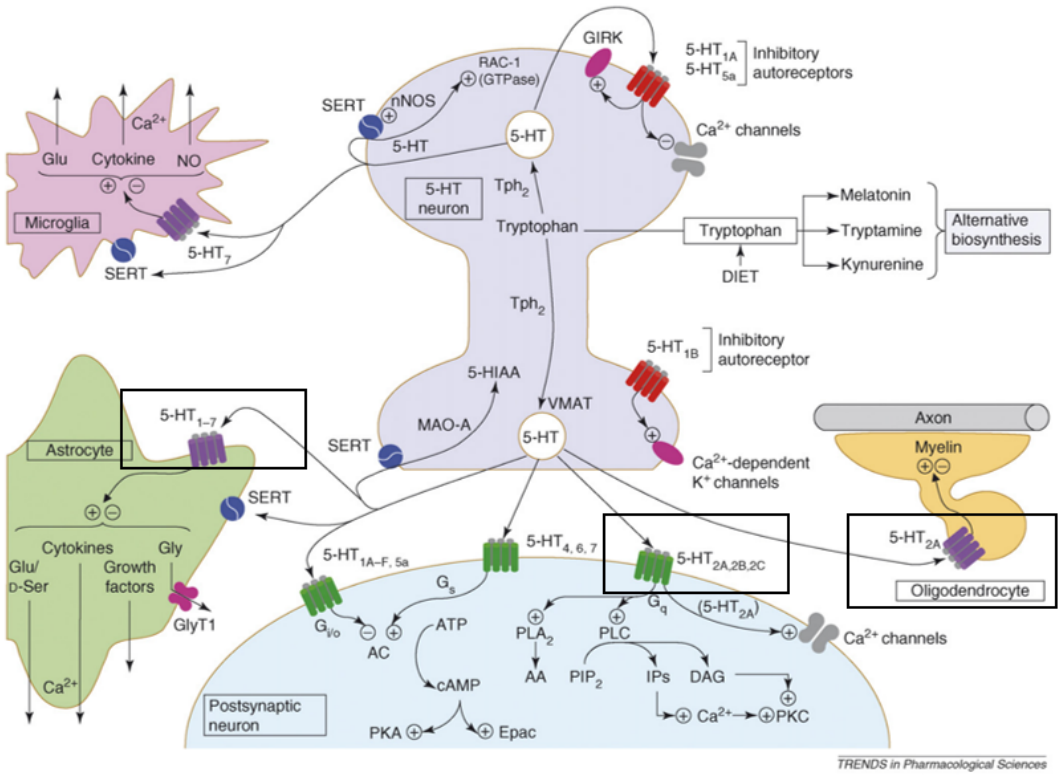

Figure 22. 5-HT Receptors Act on a Wide Range of Cellular Processes
Figure adapted from Millan et al. (2008). 5-HT receptors are found in a range of cell types and mediate a range of signaling pathways. Notice the presence of 5-HT2A receptors in neurons, as well as in astrocytes and oligodendrocytes (marked with boxes).

understanding their function in the cell could lead to discoveries in a broad range of fields (Raymond et al. 2001, Millan et al. 2008, Figure 22).

Before these modified plasmids can be used for additional research, two important points must be addressed. First is the expression of the 5-HT2BR+mCherry receptor protein. Because the receptor did not seem to properly traffic to the cell membrane, or at least not as consistently as was seen in the 5-HT2AR+EBFP and 5-HT2CR+EGFP receptors, determining a way to modify the sequence so the fluorescent tag is less inhibitory may be needed for proper evaluation of

receptor function. It is possible that using another fluorescent protein tag, such as TdTomato, might produce differing results, however mCherry was selected because of its specific excitation and emission spectra to reduce overlap with the other two fluorophores, so minimizing any overlap should be maintained in subsequent modifications. Secondly, time should be carefully considered when working with these cell lines. Because full expression of the 5-HT2R is not seen until 24 hours after induction with doxycycline, experiments are somewhat more limited than initially expected. These cells would not be effective for experiments examining the result of immediate expression of 5-HT2Rs on a cellular process, but are quite effective in other respects, as long as this induction time is factored into experimental design.

This study was an important exploration into the use of fluorescent protein tags for identifying G-protein coupled receptors. It is possible that tagging does affect receptor function in some respects, especially if there is activity at the C-terminus of the receptor, but for the purposes of JCPyV binding and interaction studies, this model appears to be sufficient to gain an understanding of 5-HT2R interactions with the addition of more data. While immunochemistry would be faster and less time-consuming for identifying receptor location, the lack of specific antibodies against the 5-HT2R subtypes is problematic. With the stable expression of 5-HT2Rs in live cells, the entire fixation step can be bypassed, which is optimal for experiments where fixation could alter the physiology of the cell. Overall, while the main purpose of the modified 5-

HT2Rs generated here is in determining JCPyV biology during cell infection, the receptors have application in a wide range of other areas as well. With the addition of more significant colocalization data, it is possible that an understanding of JCPyV interactions with 5-HT2Rs could be reached which could lead to potential therapeutic targets through which to relieve or prevent PML for those affected or at risk.

References

Aksamit AJ, Major EO, Ghatak NR, Sidhu GS, Parisi JE, Guccion JG. Diagnosis of progressive multifocal leukoencephalopathy by brain biopsy with biotin labeled DNA: DNA in situ hybridization. Journal of Neuropathology and Experimental Neurology (1987). 46 (5): 556–566. DOI: 10.1097/00005072-198709000-00005.

Assetta B, Atwood WJ. The Biology of JC Polyomavirus. Biological Chemistry (2017). 398 (8): 1-17. DOI: 10.1515/hsz-2016-0345.

Assetta B, Maginnis MS, Gracia Ahufinger I, Haley SA, Gee GV, Nelson CD, O'Hara BA, Allen Ramdial SA, Atwood WJ. 5-HT2 receptors facilitate JC polyomavirus entry. Journal of Virology (2013). 87 (24): 13490–13498. DOI: 10.1128/JVI.02252-13.

Assetta B, Morris-Love J, Gee GV, Atkinson AL, O'Hara BA, Haley SA, Atwood WJ. Genetic and Functional Dissection of the Role of Individual 5-HT2 Receptors as Entry Receptors for JC polyomavirus. Cell Reports (2019). In press.

Astrom KE, Mancall EL, Richardson EP Jr. Progressive multifocal leukoencephalopathy; a hitherto unrecognized complication of chronic lymphatic leukaemia and Hodgkin's disease. Brain (1958). 81:93–111.

Balduzzi A, Lucchini G, Hirsch HH, Basso S, Cioni M, Rovelli A, Zincone A, Grimaldi M, Corti P, Bonanomi S, Biondi A, Locatelli F, Biagi E, Comoli P. Polyomavirus JC-targeted T-

cell therapy for progressive multiple leukoencephalopathy in a hematopoietic cell transplantation recipient. Bone Marrow Transplantation (2011). 46 (7): 987-992. DOI: 10.1038/bmt.2010.221.

Dunn KW, Kamocka MM, McDonald JH. A practical guide to evaluating colocalization in biological microscopy. American Journal of Physiology: Cell Physiology (2011). 300 (4): C723-42. DOI: 10.1152/ajpcell.00462.2010.

Elphick GF, Querbes W, Jordan JA, Gee GV, Eash S, Manley K, Dugan A, Stanifer M, Bhatnagar A, Kroeze WK, Roth BL, Atwood WJ. The human polyomavirus, JCV, uses serotonin receptors to infect cells. Science (2004). 306 (5700), 1380–1383. DOI: 10.1126/science.1103492.

Faron-Gorecka A, Szlachta M, Kolasa M, Solich J, Gorecki A, Kusmider M, Zurewek D, Dziedzicka-Wasylewska M. Understanding GPCR Dimerization. In: Shukla KA, editor. Methods in Cell Biology (2019). Chapter 10. 149: 155-178. DOI: 10.1016/bs.mcb.2018.08.005.

Ferenczy MW, Marshall LJ, Nelson CD, Atwood WJ, Nath AJ, Khalili K, Major EO. Molecular biology, epidemiology, and pathogenesis of progressive multifocal leukoencephalopathy, the JC virus-induced demyelinating disease of the human brain. Clinical Microbiology Review (2012). 25 (3): 475-506. DOI:

10.1128/CMR.05031-11.

Haley SA, O'Hara BA, Nelson CD, Brittingham FL, Henriksen KJ, Stopa EG, Atwood WJ. Human polyomavirus receptor distribution in brain parenchyma contrasts with receptor distribution in kidney and choroid plexus. American Journal of Pathology (2015). 185 (8): 2246–2258. DOI: 10.1016/j.ajpath.2015.04.003.

Haley SH, Atwood WJ. Progressive Multifocal Leukoencephalopathy: Endemic Viruses and Lethal Brain Disease. Annual Review of Virology (2017). 4 (1): 349-367. DOI: 10.1146/annurev-virology-101416-041439.

Kean JM, Rao S, Wang M, Garcea RL. Seroepidemiology of human polyomaviruses. PLoS Pathogen (2009). 5: e1000363. DOI: 10.1371/journal.ppat.1000363

Killham L. Isolation in suckling mice of a virus from C3H mice harbouring Bittner milk agent. Science (1952). 116 (3015): 391-392. DOI: 10.1126/science.116.3015.391

Knowles WA, Pipkin P, Andrews N, Vyse A, Minor P, Brown DW, Miller E. Population-based study of antibody to the human polyomaviruses BKV and JCV and the simian polyomavirus SV40. Journal of Medical Virology (2003). 71 (1): 115-123. DOI: 10.1002/jmv.10450.

Kondo Y, Windrem MS, Zou L, Chandler-Militello D, Schanz SJ, Auvergne RM, Betstadt SJ, Harrington AR, Johnson M, Kazarov A, Gorelik L, Goldman SA. Human glial chimeric

mice reveal astrocytic dependence of JC virus infection. Journal of Clinical Investigation (2014). 124 (12): 5323–36. DOI: 10.1172/JCI76629.

Koralnik IJ, Du Pasquier RA, Kuroda MJ, Schmitz JE, Dang X, Zheng Y, Lifton M, Letvin NL. Association of prolonged survival in HLA-A2 + progressive multifocal leukoencephalopathy patients with a CTL response specific for a commonly recognized JC virus epitope. Journal of Immunology (2002). 168 (1), 499–504. DOI: 10.4049/jimmunol.168.1.499.

Lukasiewicz S, Blasiak E, Dzeidzicka-Wasylewska M. 5-HT2 Receptor Heterodimerization. In: Guiard BP, Giovanni GV., editor. 5-HT2 Receptors in the Central Nervous System. Springer; 2018. 57-66. ISBN: 3319704745, 9783319704746.

Maginnis MS, Haley SA, Gee GV, Atwood WJ. Role of N-linked glycosylation of the 5-HT2A receptor in JC virus infection. Journal of Virology (2010). 84 (19): 9677–9684. DOI: 10.1128/JVI.00978-10.

Major EO. Progressive multifocal leukoencephalopathy in patients on immunomodulatory therapies. Annual Review of Medicine (2010). 61: 35-47. DOI: 10.1146/annurev.med.080708.082655.

Manders EMM, Verbeek FJ, Aten JA. Measurement of co-localization of objects in dual-color confocal images. Journal of Microscopy (1993). 169 (3): 375-382. DOI:

10.1111/j.1365-2818.1993.tb03313.x.

Marshall LJ, Ferenczy MW, Daley EL, Jensen PN, Ryschkewitsch CF, Major EO. Lymphocyte gene expression and JC virus noncoding control region sequences are linked with the risk of progressive multifocal leukoencephalopathy. Journal of Virology (2014). 88: 5177–83.

Millan MJ, Marin P, Bockaert J, Mannoury la Cour C. Signaling at G-protein-coupled serotonin receptors: recent advances and future research directions. Trends in Pharmacological Sciences (2008). 29 (9): 454-464. DOI: 10.1016/j.tips.2008.06.007.

Morris-Love J, Gee GV, O'Hara BA, Assetta B, Atkinson AL, Dugan AS, Haley SA, Atwood WA. JC polyomavirus uses Extracellular Vesicles to Infect Target Cells. mBio (2019). In press.

NEBuilder® HiFi DNA Assembly Master Mix/NEBuilder HiFi DNA Assembly Cloning Kit Instruction Manual. New England BioLabs Inc. (2017). Web Accessed < https://www.neb.com/-/media/catalog/datacards-or-manuals/manuale5520.pdf?rev=e68bf93062424c9fb30c51aef30fe48c>.

Neu U, Maginnis MS, Palma AS, Stroh LJ, Nelson CD, Feizi T, Atwood WJ, Stehle T. Structure-function analysis of the human JC polyomavirus establishes the LSTc pentasaccharide as a functional receptor motif. Cell Host Microbe (2010). 8 (4): 309–

319. DOI: 10.1016/j.chom.2010.09.004.

Padgett BL, Walker DL, ZuRhein GM, Eckroade RJ, Dessel BH. Cultivation of papova-like virus from human brain with progressive multifocal leucoencephalopathy. Lancet (1971). 1 (7712): 1257-1260. DOI: 10.1016/S0140-6736(71)91777-6.

Padgett BL, Walker DL. Prevalence of antibodies in human sera against JC virus, an isolate from a case of progressive multifocal leukoencephalopathy. Journal of Infectious Disease (1973). 127 (4):467-470. DOI: 10.1093/infdis/127.4.467.

Pelosini M, Focosi D, Rita F, Galimberti S, Caracciolo F, Benedetti E, Papineschi F, Petrini M. Progressive multifocal leukoencephalopathy: report of three cases in HIV-negative hematological patients and review of literature. Annals of Hematology (2008). 87 (5): 405-412. DOI: 10.1007/s00277-007-0411-6.

Pho MT, Ashok A, Atwood WJ. JC virus enters human glial cells by clathrin-dependent receptor-mediated endocytosis. Journal of Virology (2000). 74 (5): 2288–2292. DOI: 10.1128/JVI.74.5.2288-2292.2000.

Pinto M, Dobson S. BK and JC virus: A review. Journal of Infection (2014). 68: S2-S8. DOI: 10.1016/j.jinf.2013.09.009.

Querbes W, Benmerah A, Tosoni D, Di Fiore PP, Atwood WJ. A JC virus-induced signal is required for infection of glial cells by a clathrin- and eps15-dependent pathway.

Journal of Virology (2004). 78 (1): 250–256. DOI: 10.1128/JVI.78.1.250-256.2004.

Querbes W, O'Hara BA, Williams G, Atwood WJ. Invasion of host cells by JC virus identifies a novel role for caveolae in endosomal sorting of noncaveolar ligands. Journal of Virology (2006). 80 (19): 9402–9413. DOI: 10.1128/JVI.01086-06.

Raote I, Bhattacharya A, Panicker MM. Serotonin 2A (5-HT2A) Receptor Function: Ligand-Dependent Mechanisms and Pathways. In: Chattopadhyay A, editor. Serotonin Receptors in Neurobiology. Boca Raton (FL): CRC Press/Taylor & Francis; 2007. Chapter 6. Available from: https://www.ncbi.nlm.nih.gov/books/NBK1853/#

Raymond JR, Mukhin YV, Gelasco A, Turner J, Collinsworth G, Gettys TW, Grewalb JS, Garnovskaya MN. Multiplicity of mechanisms of serotonin receptor signal transduction. Pharmacology and Therapeutics (2001). 92 (2-3): 179-212. DOI: 10.1016/S0163-7258(01)00169-3.

Richardson EP Jr. Progressive Multifocal Leukoencephalopathy. New England Journal of Medicine (1961). 265:815-823. DOI: 10.1056/NEJM196110262651701

Sacktor N. The epidemiology of human immunodeficiency virus–associated neurological disease in the era of highly active antiretroviral therapy. Journal of Neurovirology (2002). 8 (Suppl. 2): 115–121. DOI: 10.1080/13550280290101094.

Steiner I, Berger JR. Update on progressive multifocal leukoencephalopathy. Current

Neurology and Neuroscience Reports (2012). 12 (6): 680–686. DOI: 10.1007/s11910-012-0313-4.

Tet-On® Advanced Inducible Gene Expression Systems User Manual. ClonTech Laboratories, Inc. (2012). Protocol No. PT3898-1, Version No. 102312.

White FA III, Ishaq M, Stoner GL, Frisque RJ. JC virus DNA is present in many human brain samples from patients without progressive multifocal leukoencephalopathy. Journal of Virology (1992). 66:5726–34.

White MK and Khalili K. Pathogenesis of progressive multifocal leukoencephalopathy revisited. Journal of Infectious Disease (2011). 203 (5): 578–586. DOI: 10.1093/infdis/jiq097.

Supplemental Information

Gateway Modified Primers

Letter case (A vs. a) indicates switch from vector-specific to insert-specific sequence.

5-HT2AR+EBFP

Includes His Tag in sequence

FORWARD: 5’ gcatggacgagctgtacaagCACCACCACCACCACCAC 3’

REVERSE: 5’ tcttcacaaagaatatccatGCTAGCCAATTCTCCAGG 3’

5-HT2BR+mCherry

Does not include His Tag

FORWARD: 5’ tggacgagctgtacaagtaaCACCACCACCACCACCAC 3’

REVERSE: 5’ actctgtaagagagagccatGCTAGCCAATTCTCCAGG 3’

5-HT2CR+EGFP

Does not include His Tag

FORWARD: 5’ tggacgagctgtacaagtaaCACCACCACCACCACCAC 3’

REVERSE: 5’ gcattcctcaggttcaccatGCTAGCCAATTCTCCAGG 3’

Insert Sequences

Fluorescent Tag is **bold** and printed in the color corresponding to emission wavelength.

5-HT2AR+EBFP *(5-HT2AR: 1413 bp, EBFP: 717 bp, Combined: 2130 bp)*

ATGGATATTCTTTGTGAAGAAAATACTTCTTTGAGCTCAACTACGAACTCCCTAATGCAATTAA

ATGATGACACCCGATTGTATTCAAATGATTTCAACTCCGGAGAAGCTAACACTTCTGATGCAT

TTAACTGGACAGTCGACTCTGAAAATCGAACCAACCTTTCCTGTGAAGGGTGCCTCTCACC

GTCGTGTCTCTCCTTACTTCATCTCCAGGAAAAAAACTGGTCTGCTTTACTGACAGCCGTAG

TGATTATTCTAACTATTGCTGGAAACATACTCGTCATCATGGCAGTGTCCCTAGAGAAAAAGC

TGCAGAATGCCACCAACTATTTCCTGATGTCACTTGCCATAGCTGATATGCTGCTGGGTTTC

CTTGTCATGCCCGTGTCCATGTTAACCATCCTGTATGGGTACCGGTGGCCTCTGCCGAGCA

AGCTTTGTGCAGTCTGGATTTACCTGGACGTGCTCTTCTCCACGGCCTCCATCATGCACCT

CTGCGCCATCTCGCTGGACCGCTACGTCGCCATCCAGAATCCCATCCACCACAGCCGCTTC

AACTCCAGAACTAAGGCATTTCTGAAAATCATTGCTGTTTGGACCATATCAGTAGGTATATCC

ATGCCAATACCAGTCTTTGGGCTACAGGACGATTCGAAGGTCTTTAAGGAGGGGAGTTGCT

TACTCGCCGATGATAACTTTGTCCTGATCGGCTCTTTTGTGTCATTTTTCATTCCCTTAACCAT

CATGGTGATCACCTACTTTCTAACTATCAAGTCACTCCAGAAAGAAGCTACTTTGTGTGTAAG

TGATCTTGGCACACGGGCCAAATTAGCTTCTTTCAGCTTCCTCCCTCAGAGTTCTTTGTCTT

CAGAAAAGCTCTTCCAGCGGTCGATCCATAGGGAGCCAGGGTCCTACACAGGCAGGAGGA

CTATGCAGTCCATCAGCAATGAGCAAAAGGCATGCAAGGTGCTGGGCATCGTCTTCTTCCT

GTTTGTGGTGATGTGGTGCCCTTTCTTCATCACAAACATCATGGCCGTCATCTGCAAAGAGT

CCTGCAATGAGGATGTCATTGGGGCCCTGCTCAATGTGTTTGTTTGGATCGGTTATCTCTCT

TCAGCAGTCAACCCACTAGTCTACACACTGTTCAACAAGACCTATAGGTCAGCCTTTTCACG

GTATATTCAGTGTCAGTACAAGGAAAACAAAAAACCATTGCAGTTAATTTTAGTGAACACAATA

CCGGCTTTGGCCTACAAGTCTAGCCAACTTCAAATGGGACAAAAAAAGAATTCAAAGCAAGA

TGCCAAGACAACAGATAATGACTGCTCAATGGTTGCTCTAGGAAAGCAGCATTCTGAAGAG

GCTTCTAAAGACAATAGCGACGGAGTGAATGAAAAGGTGAGCTGTGTG**GTGAGCAAGGGC**

GAGGAGCTGTTCACCGGGGTGGTGCCCATCCTGGTCGAGCTGGACGGCGACGTAAACG

GCCACAAGTTCAGCGTGAGGGGCGAGGGCGAGGGCGATGCCACCAACGGCAAGCTGA

CCCTGAAGTTCATCAGTACTACCGGCAAGCTGCCCGTGCCCTGGCCCACCCTCGTGACC

ACCCTGAGCCACGGCGTGCAGGTGTTCGCCCGCTACCCCGACCACATGAAGCAGCACG

ACTTCTTCAAGTCCGCCATGCCCGAAGGCTACGTCCAGGAGCGCACCATCTTCTTCAAG

GACGACGGCACCTACAAGACCCGCGCCGAGGTGAAGTTCGAGGGCGACACCCTGGTGA

ACCGCATCGAGCTGAAGGGCGTCGACTTCAAGGAGGACGGCAACATCCTGGGGCACAA

GCTGGAGTACAACTTCAACAGCCACAACATCTATATCATGGCCGTCAAGCAGAAGAACG

GCATCAAGGCCAACTTCAAGATCCGCCACAACGTGGAGGACGGCAGCGTGCAGCTCGC

CGACCACTACCAGCAGAACACCCCCATCGGCGACGGCCCCGTGCTGCTGCCCGACAGC

CACTACCTGAGCACCCAGTCCAAGCTTAGCAAAGACCCCAACGAGAAGCGCGATCACAT

GGTCCTGCTGGAGTTCCGCACCGCCGCCGGGATCACTCTCGGCATGGACGAGCTGTACA

AGTAA

5-HT2BR+mCherry *(5-HT2BR: 1443 bp, mCherry: 708 bp, Combined: 2151 bp)*

ATGGCTCTCTCTTACAGAGTGTCTGAACTTCAAAGCACAATTCCTGAGCACATTTTGCAGAG

CACCTTTGTTCACGTCATAAGTTCCAATTGGAGTGGATTACAGACAGAATCAATACCAGAGG

AAATGAAACAGATTGTTGAGGAACAGGGAAATAAACTGCACTGGGCAGCTCTTCTGATACT

CATGGTGATAATACCCACAATTGGTGGAAATACCCTTGTTATTCTGGCTGTTTCACTGGAGA

AGAAGCTGCAGTATGCTACTAATTACTTTCTAATGTCCTTGGCGGTGGCTGATTTGCTGGTT

GGATTGTTTGTGATGCCAATTGCCCTCTTGACAATAATGTTTGAGGCTATGTGGCCCCTCC

CACTTGTTCTATGTCCTGCCTGGTTATTTCTTGACGTTCTCTTTTCAACCGCATCCATCATG

CATCTCTGTGCCATTTCAGTGGATCGTTACATAGCCATCAAAAAGCCAATCCAGGCCAATC

AATATAACTCACGGGCTACAGCATTCATCAAGATTACAGTGGTGTGGTTAATTTCAATAGGC

ATTGCCATTCCAGTCCCTATTAAAGGGATAGAGACTGATGTGGACAACCCAAACAATATCA

CTTGTGTGCTGACAAAGGAACGTTTTGGCGATTTCATGCTCTTTGGCTCACTGGCTGCCTT

CTTCACACCTCTTGCAATTATGATTGTCACCTACTTTCTCACTATCCATGCTTTACAGAAGAA

GGCTTACTTAGTCAAAAACAAGCCACCTCAACGCCTAACATGGTTGACTGTGTCTACAGTTT

TCCAAAGGGATGAAACACCTTGCTCGTCACCGGAAAAGGTGGCAATGCTGGATGGTTCTC

GAAAGGACAAGGCTCTGCCCAACTCAGGTGATGAAACACTTATGCGAAGAACATCCACAAT

TGGGAAAAAGTCAGTGCAGACCATTTCCAACGAACAGAGAGCCTCAAAGGTCCTAGGGAT

TGTGTTTTTCCTCTTTTTGCTTATGTGGTGTCCCTTCTTTATTACAAATATAACTTTAGTTTTA

TGTGATTCCTGTAACCAAACTACTCTCCAAATGCTCCTGGAGATATTTGTGTGGATAGGCTA

TGTTTCCTCAGGAGTGAATCCTTTGGTCTACACCCTCTTCAATAAGACATTTCGGGATGCAT

TTGGCCGATATATCACCTGCAATTACCGGGCCACAAAGTCAGTAAAAACTCTCAGAAAACG

CTCCAGTAAGATCTACTTCCGGAATCCAATGGCAGAGAACTCTAAGTTTTTCAAGAAACATG

GAATTCGAAATGGGATTAACCCTGCCATGTACCAGAGTCCAATGAGGCTCCGAAGTTCAAC

CATTCAGTCTTCATCAATCATTCTACTAGATACGCTTCTCCTCACTGAAAATGAAGGTGACA

AAACTGAAGAGCAAGTTAGTTATGTA**GTGAGCAAGGGCGAGGAGGATAACATGGCCATC**

ATCAAGGAGTTCATGCGCTTCAAGGTGCACATGGAGGGCTCCGTGAACGGCCACGAGTT

CGAGATCGAGGGCGAGGGCGAGGGCCGCCCCTACGAGGGCACCCAGACCGCCAAGCT

GAAGGTGACCAAGGGTGGCCCCCTGCCCTTCGCCTGGGACATCCTGTCCCCTCAGTTCA

TGTACGGCTCCAAGGCCTACGTGAAGCACCCCGCCGACATCCCCGACTACTTGAAGCTG

TCCTTCCCCGAGGGCTTCAATTGGGAGCGCGTGATGAACTTCGAGGACGGCGGCGTGGT

GACCGTGACCCAGGACTCCTCCCTGCAGGACGGCGAGTTCATCTACAAGGTGAAGCTGC

GCGGCACCAACTTCCCCTCCGACGGCCCCGTAATGCAGTGTCGTACCATGGGCTGGGAG

GCCTCCACTGAGCGGATGTACCCCGAGGACGGCGCCCTGAAGGGCGAGATCAAGCAGA

GGCTGAAGCTGAAGGACGGCGGCCACTACGACGCTGAGGTCAAGACCACCTACAAGGC

CAAGAAGCCCGTGCAGCTGCCCGGCGCCTACAACGTCGACATCAAGTTGGACATCCTTT

CCCACAACGAGGACTACACCATCGTGGAACAGTACGAACGCGCCGAGGGCCGCCACTC

CACCGGCGGCATGGACGAGCTGTACAAGTAA

5-HT2CR+EGFP *(5-HT2CR: 1374 bp, EGFP: 717 bp, Combined: 2091 bp)*

ATGGTGAACCTGAGGAATGCGGTGCATTCATTCCTTGTGCACCTAATTGGCCTATTGGTTTG

GCAATGTGATATTTCTGTGAGCCCAGTAGCAGCTATAGTAACTGACATTTTCAATACCTCCGA

TGGTGGACGCTTCAAATTCCCAGACGGGGTACAAAACTGGCCAGCACTTTCAATCGTCATC

ATAATAATCATGACAATAGGTGGCAACATCCTTGTGATCATGGCAGTAAGCATGGAAAAGAAA

CTGCACAATGCCACCAATTACTTCTTAATGTCCCTAGCCATTGCTGATATGCTAGTGGGACTA

CTTGTCATGCCCCTGTCTCTCCTGGCAATCCTTTATGATTATGTCTGGCCACTACCTAGATAT

TTGTGCCCCGTCTGGATTTCTTTAGATGTTTTATTTTCAACAGCGTCCATCATGCATCTTTGT

GCCATTTCCCTGGATCGGTATGTAGCAATACGTAATCCTATTGAGCATAGCCGTTTCAATTC

GCGGACTAAGGCCATCATGAAGATTGCTATTGTTTGGGCAATTTCTATAGGTGTATCAGTTC

CTATCCCTGTGATTGGACTGAGGGACGAAGAAAAGGTGTTCGTGAACAACACGACGTGCG

TGCTCAACGACCCAAATTTCGTTCTTATTGGGTCCTTCGTAGCTTTCTTCATACCGCTGACG

ATTATGGTGATTACGTATTGCCTGACCATCTACGTTCTGCGCCGACAAGCTTTGATGTTACT

GCACGGCCACACCGAGGAACCGCCTGGACTAAGTCTGGATTTCCTGAAGTGCTGCAAGAG

GAATACGGCCGAGGAAGAGAACTCTGCAAACCCTAACCAAGACCAGAACGCACGCCGAAG

AAAGAAGAAGGAGAGACGTCCTAGGGGCACCATGCAGGCTATCAACAATGAAAGAAAAGC

TTCGAAAGTCCTTGGGATTGTTTTCTTTGTGTTTCTGATCATGTGGTGCCCATTTTTCATTAC

CAATATTCTGTCTGTTCTTTGTGAGAAGTCCTGTAACCAAAAGCTCATGGAAAAGCTTCTGA

ATGTGTTTGTTTGGATTGGCTATGTTTGTTCAGGAATCAATCCTCTGGTGTATACTCTGTTC

AACAAAATTTACCGAAGGGCATTCTCCAACTATTTGCGTTGCAATTATAAGGTAGAGAAAAA

GCCTCCTGTCAGGCAGATTCCAAGAGTTGCCGCCACTGCTTTGTCTGGGAGGGAGCTTAA

TGTTAACATTTATCGGCATACCAATGAACCGGTGATCGAGAAAGCCAGTGACAATGAGCCC

GGTATAGAGATGCAAGTTGAGAATTTAGAGTTACCAGTAAATCCCTCCAGTGTGGTTAGCG

AAAGGATTAGCAGTGTG**GTGAGCAAGGGCGAGGAGCTGTTCACCGGGGTGGTGCCCATC**

CTGGTCGAGCTGGACGGCGACGTAAACGGCCACAAGTTCAGCGTGTCCGGCGAGGGCG

AGGGCGATGCCACCTACGGCAAGCTGACCCTGAAGTTCATCTGCACCACCGGCAAGCTG

CCCGTGCCCTGGCCCACCCTCGTGACCACCCTGACCTACGGCGTGCAGTGCTTCAGCCG

CTACCCCGACCACATGAAGCAGCACGACTTCTTCAAGTCCGCCATGCCCGAAGGCTACG

TCCAGGAGCGCACCATCTTCTTCAAGGACGACGGCAACTACAAGACCCGCGCCGAGGT

GAAGTTCGAGGGCGACACCCTGGTGAACCGCATCGAGCTGAAGGGCATCGACTTCAAG

GAGGACGGCAACATCCTGGGGCACAAGCTGGAGTACAACTACAACAGCCACAACGTCT

ATATCATGGCCGACAAGCAGAAGAACGGCATCAAGGTGAACTTCAAGATCCGCCACAAC

ATCGAGGACGGCAGCGTGCAGCTCGCCGACCACTACCAGCAGAACACCCCCATCGGCG

ACGGCCCCGTGCTGCTGCCCGACAACCACTACCTGAGCACCCAGTCCAAGCTGAGCAA

AGACCCCAACGAGAAGCGCGATCACATGGTCCTGCTGGAGTTCGTGACCGCCGCCGGG

ATCACTCTCGGCATGGACGAGCTGTACAAGTAA

Validation Primers

5-HT2AR+EBFP

FORWARD: “LNCX” 5’ AGCTCGTTTAGTGAACCGTCAGATC 3’

5’ GATCGCCTGGAGAATTGGCT 3’

REVERSE: 5’ GTGGAGAAGAGCACGTCCAG 3’

5-HT2BR+mCherry

FORWARD: “LNCX” 5’ AGCTCGTTTAGTGAACCGTCAGATC 3’

5’ GATCGCCTGGAGAATTGGCT 3’

REVERSE: 5’ AGGGACTGGAATGGCAATGC 3’

5-HT2CR+EGFP

FORWARD: “LNCX” 5’ AGCTCGTTTAGTGAACCGTCAGATC 3’

5’ GATCGCCTGGAGAATTGGCT 3’

REVERSE: 5’ TCATGATGGCCTTAGTCCGC 3’

Gateway-Positive (Failed NEBuilder Reaction) Identification Primers:

FORWARD: 5’ GCCTGGAGAATTGGCTAGCA 3’

REVERSE: 5’ TCACCAGCTCACCGTCTTTC 3’

Gateway-Negative Insert-Negative (Failed NEBuilder Reaction) Identification Primers:

FORWARD: 5’ CGTATGTCGAGGTAGGCGTG 3’

REVERSE: 5’ GAACAGGGCCCACACTACC 3’

Site-Directed Mutagenesis Primers

5-HT2AR+EBFP

FORWARD: 5’ AAATGATTTCAACTCCGGAGAAGCTAAC 3’

REVERSE: 5’ GAATACAATCGGGTGTCATCATTTAATTGC 3’

5-HT2BR+mCherry

FORWARD: 5’ CAATTGGAGTGGATTACAGACAGAATCAATAC 3’

REVERSE: 5’ GAACTTATGACGTGAACAAAGGTGCTCTG 3’

5-HT2CR+EGFP

FORWARD: 5’ GCCATTTCCCTGGATCGGTATGTAGCAATAC 3’

REVERSE: 5’ ACAAAGATGCATGATGGACGCTGTTGAAAATAA 3’

Supplemental Figures

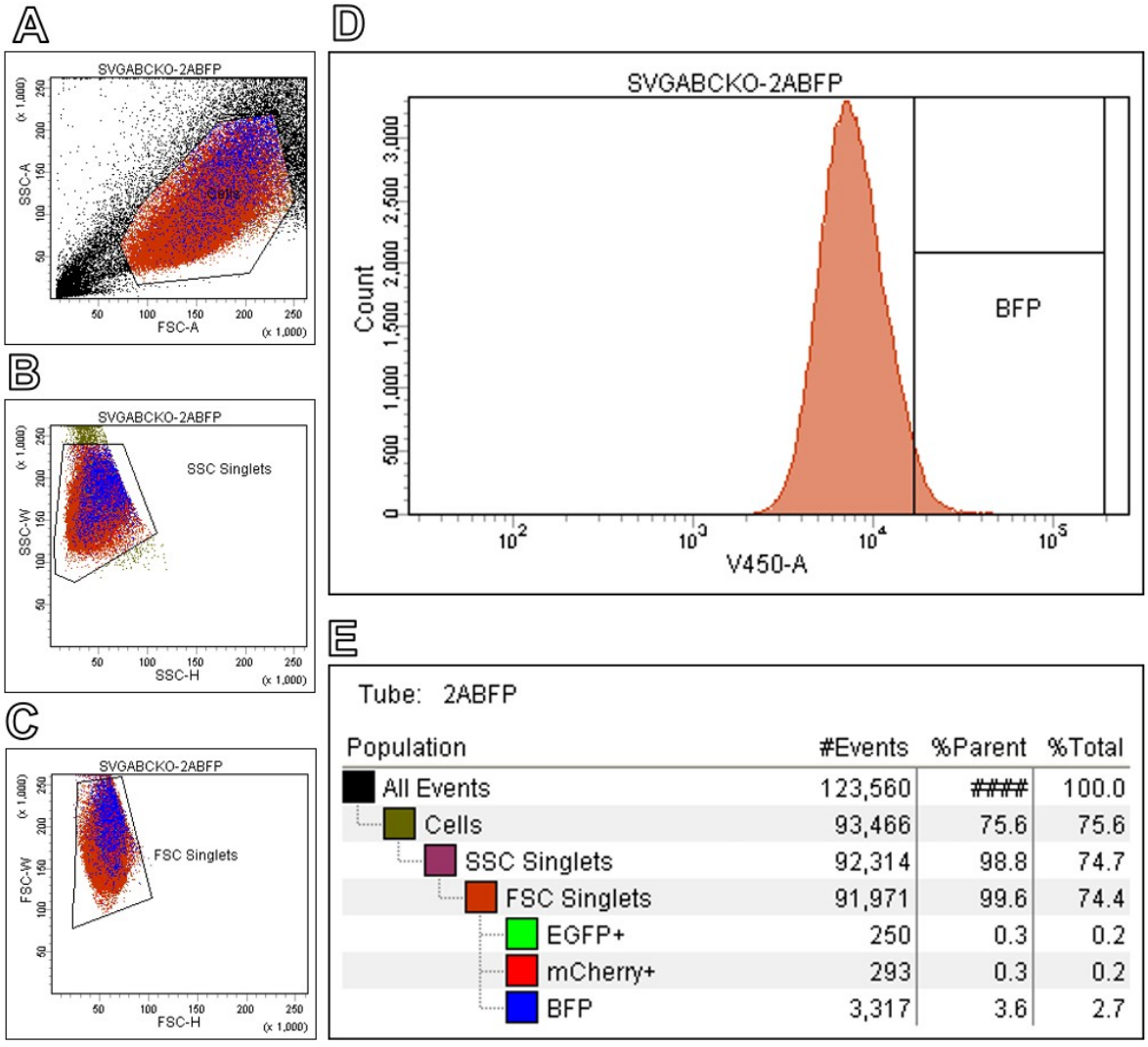

Figure S1. FACS Sorting of SVG2ABCKO Cells Stably Transduced with 5-HT2AR+EBFP
Modified pLIX_403 containing the 5-HT2AR+EBFP insert post-site-directed-mutagenesis was used to produce lentivirus for infection of SVG2ABCKO cells. Cells were selected using puromycin for 1 week with doxycycline before Flow Activated Cell Sorting. The panel above shows workflow (E), subsequent gating (A-C) and population grouping (D) steps of the cell sort. Post sorting, cells were evaluated for expression with doxycycline.

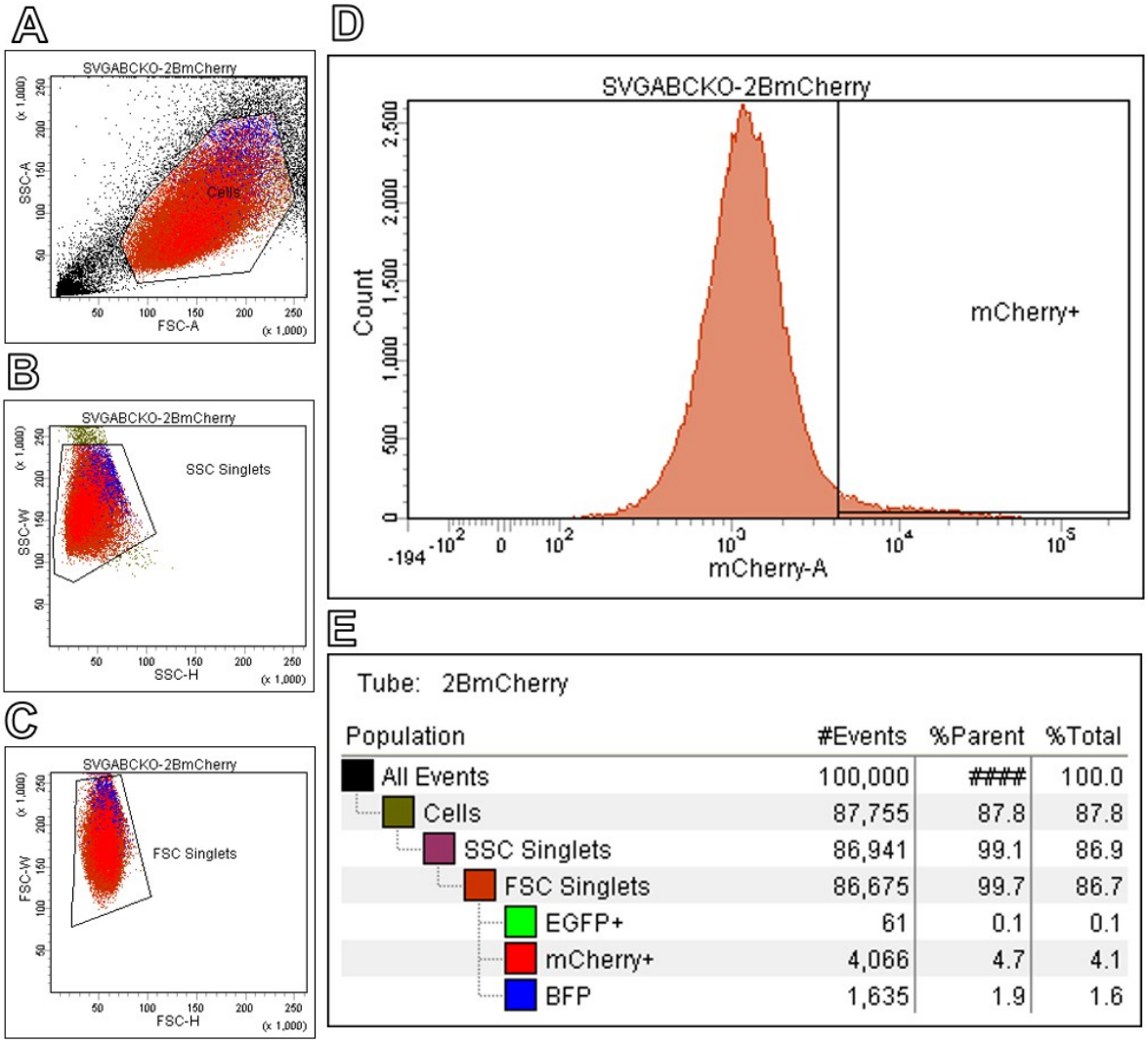

Figure S2. FACS Sorting of SVG2ABCKO Cells Stably Transduced with 5-HT2BR+mCherry
Modified pLIX_403 containing the 5-HT2BR+mCherry insert post-site-directed-mutagenesis was used to produce lentivirus for infection of SVG2ABCKO cells. Cells were selected using puromycin for 1 week with doxycycline before Flow Activated Cell Sorting. The panel above shows workflow (E), subsequent gating (A-C) and population grouping (D) steps of the cell sort. Post sorting, cells were evaluated for expression with doxycycline.

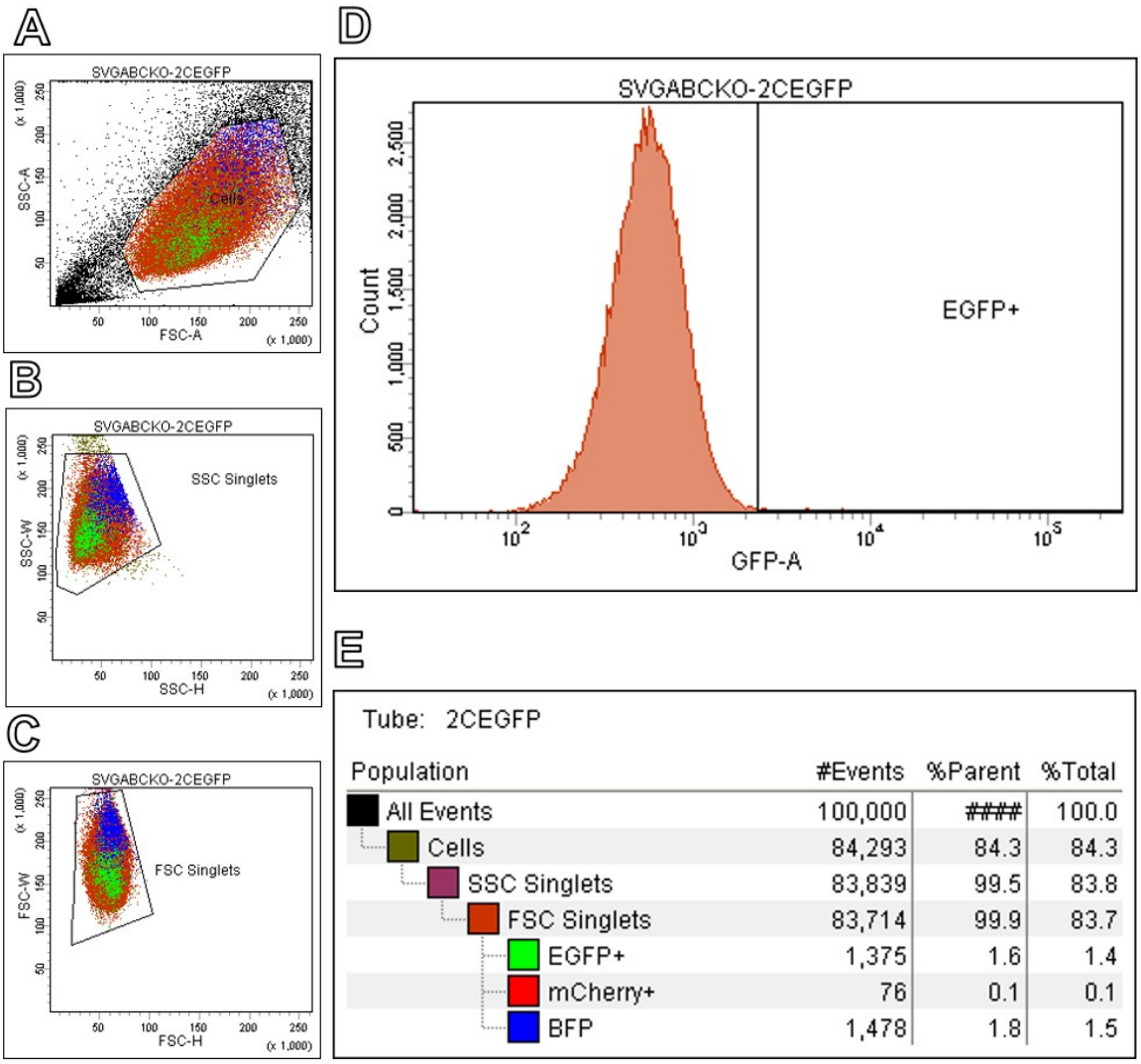

Figure S3. FACS Sorting of SVG2ABCKO Cells Stably Transduced with 5-HT2CR+EGFP
Modified pLIX_403 containing the 5-HT2CR+EGFP insert post-site-directed-mutagenesis was used to produce lentivirus for infection of SVG2ABCKO cells. Cells were selected using puromycin for 1 week with doxycycline before Flow Activated Cell Sorting. The panel above shows workflow (E), subsequent gating (A-C) and population grouping (D) steps of the cell sort. Post sorting, cells were evaluated for expression with doxycycline.

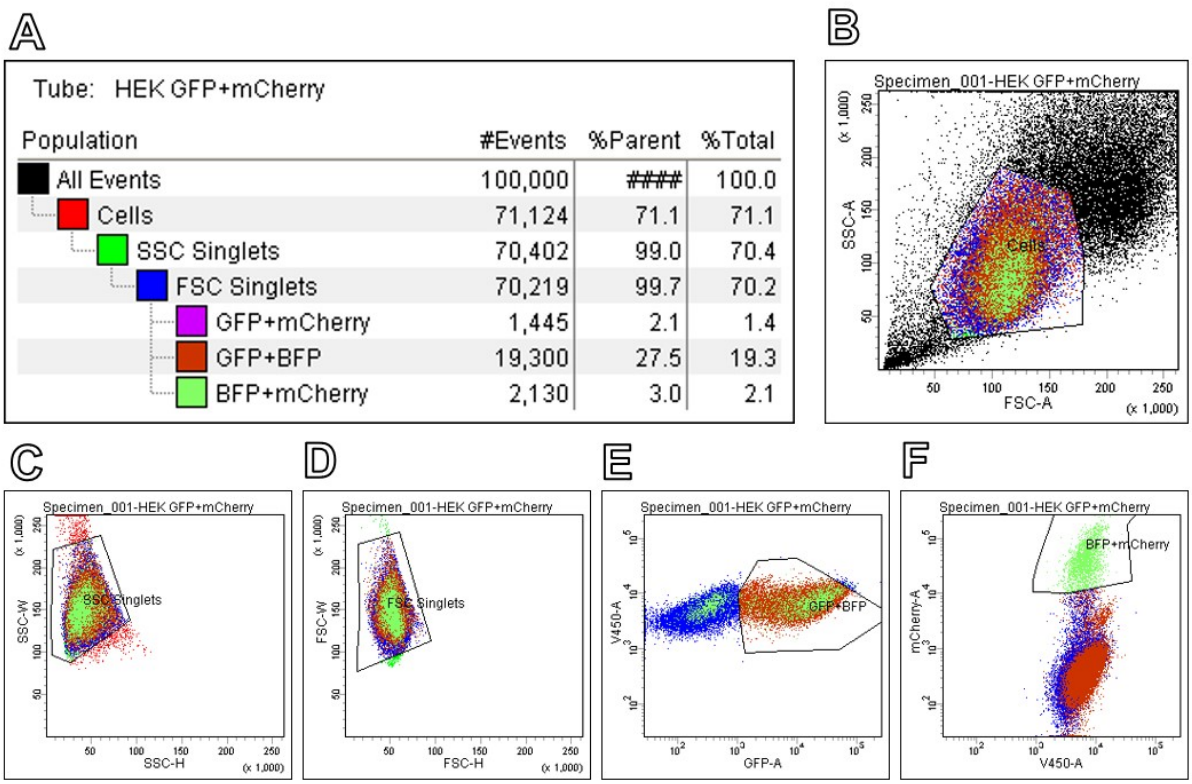

Figure S4. FACS Sorting of HEK293A Cells Stably Transduced with 5-HT2BR+mCherry and 5-HT2CR+EGFP

Modified pLIX_403 plasmids containing the 5-HT2BR+mCherry or 5-HT2CR+EGFP insert post-site-directed-mutagenesis was used to produce lentivirus for double/subsequent infection of HEK293A cells. Cells were selected using puromycin for 1 week with doxycycline before Flow Activated Cell Sorting for 5-HT2CR+EGFP, and then infected and sorted again for 5-HT2BR+mCherry. The panel above shows workflow (A) and subsequent gating (B-F) steps of the cell sort. Post sorting, cells were evaluated for expression with doxycycline.

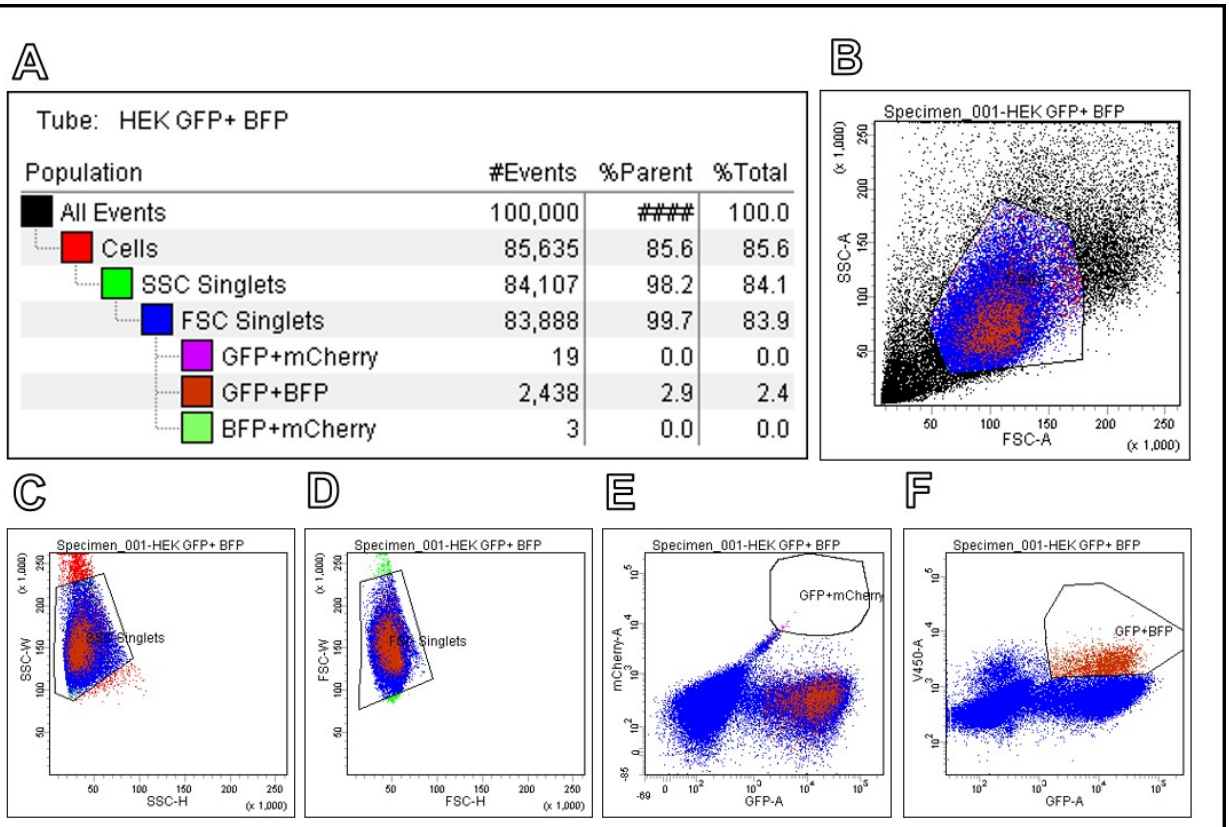

Figure S5. FACS Sorting of HEK293A Cells Stably Transduced with 5-HT2AR+EBFP and 5-HT2CR+EGFP

Modified pLIX_403 plasmids containing the 5-HT2AR+EBFP or 5-HT2CR+EGFP insert post-site-directed-mutagenesis was used to produce lentivirus for double/subsequent infection of HEK293A cells. Cells were selected using puromycin for 1 week with doxycycline before Flow Activated Cell Sorting for 5-HT2CR+EGFP, and then infected and sorted again for 5-HT2AR+EBFP. The panel above shows workflow (A) and subsequent gating (B-F) steps of the cell sort. Post sorting, cells were evaluated for expression with doxycycline.

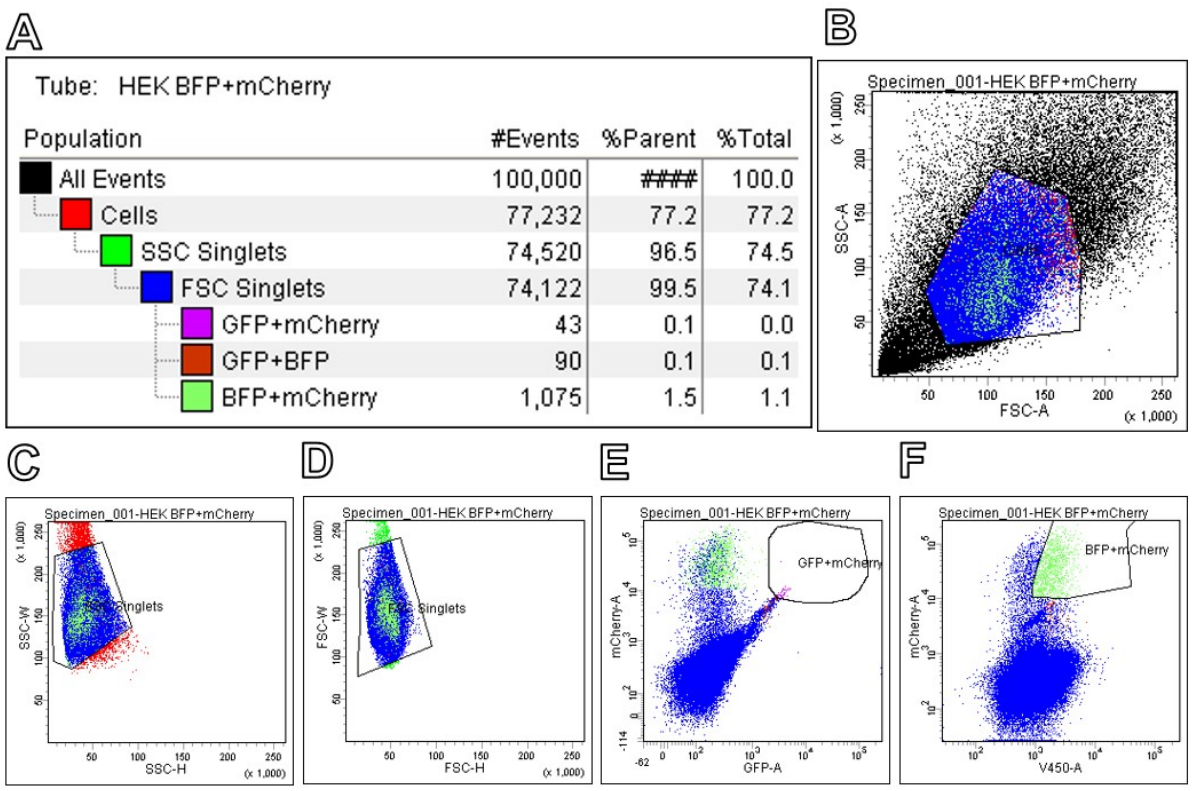

Figure S6. FACS Sorting of HEK293A Cells Stably Transduced with 5-HT2AR+EBFP and 5-HT2BR+mCherry

Modified pLIX_403 plasmids containing the 5-HT2AR+EBFP or 5-HT2BR+mCherry insert post-site-directed-mutagenesis was used to produce lentivirus for double/subsequent infection of HEK293A cells. Cells were selected using puromycin for 1 week with doxycycline before Flow Activated Cell Sorting for 5-HT2AR+EBFP, and then infected and sorted again for 5-HT2BR+mCherry. The panel above shows workflow (A) and subsequent gating (B-F) steps of the cell sort. Post sorting, cells were evaluated for expression with doxycycline.

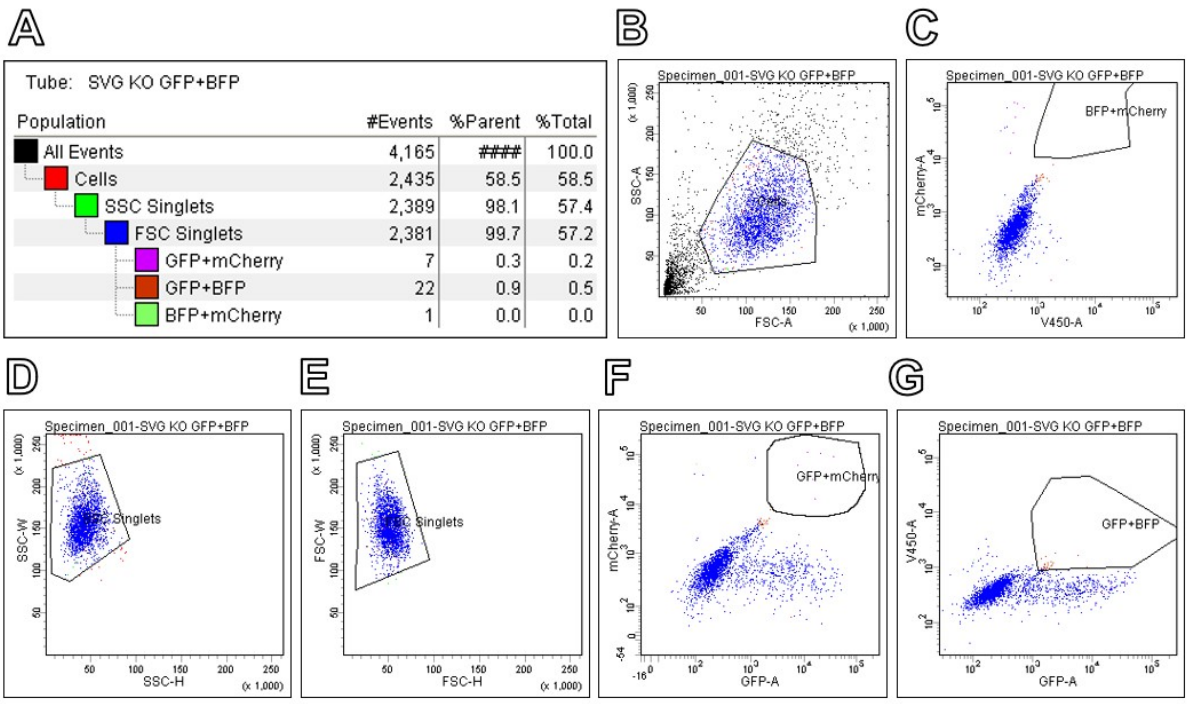

Figure S7. FACS Sorting of SVG2ABCKO Cells Stably Transduced with 5-HT2AR+EBFP and 5-HT2CR+EGFP

Modified pLIX_403 plasmids containing the 5-HT2AR+EBFP or 5-HT2CR+EGFP insert post-site-directed-mutagenesis was used to produce lentivirus for double/subsequent infection of SVG2ABCKO cells. Cells were selected using puromycin for 1 week with doxycycline before Flow Activated Cell Sorting for 5-HT2CR+EGFP, and then infected and sorted again for 5-HT2AR+EBFP. The panel above shows workflow (A) and subsequent gating (B-G) steps of the cell sort. Post sorting, cells were evaluated for expression with doxycycline. Very few to no significant events were reporting during the sort.

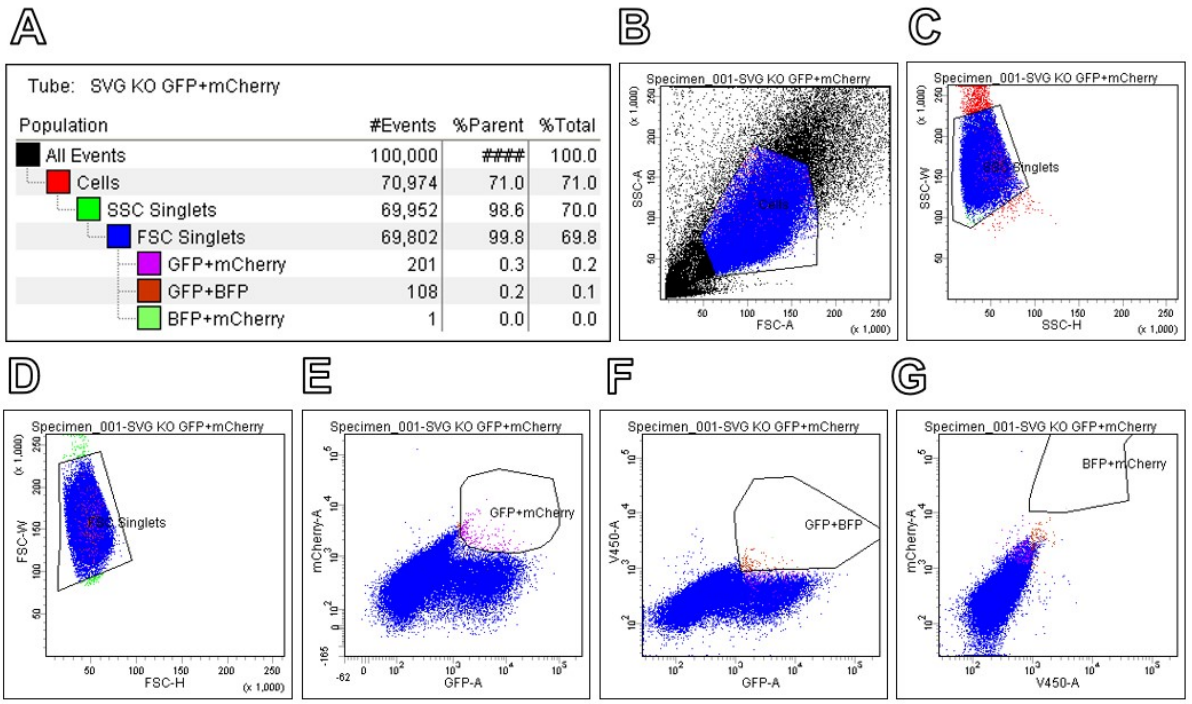

Figure S8. FACS Sorting of SVGA Cells Stably Transduced with 5-HT2BR+mCherry and 5-HT2CR+EGFP

Modified pLIX_403 plasmids containing the 5-HT2BR+mCherry or 5-T2CR+EGFP insert post-site-directed-mutagenesis was used to produce lentivirus for double/subsequent infection of SVGA cells. Cells were selected using puromycin for 1 week with doxycycline before Flow Activated Cell Sorting for 5-HT2CR+EGFP, and then infected and sorted again for 5-HT2BR+mCherry. The panel above shows workflow (A) and subsequent gating (B-G) steps of the cell sort. Post sorting, cells were evaluated for expression with doxycycline.